Review

Recent Advances and Future Perspectives in Friction Stir Welding and Processing: A Review

Dan Cătălin Bîrsan and Florin Susac *

Posted Date: 19 May 2026

doi: 10.20944/preprints202605.1246.v1

Keywords: friction stir welding (FSW); dissimilar joining; microstructural evolution; process optimization; hybrid welding

 doi:10.20944/preprints202605.1246.v1

Review

Recent Advances and Future Perspectives in Friction Stir Welding and Processing: A Review

Dan Cătălin Bîrsan and Florin Susac *

Manufacturing Engineering Department, Faculty of Engineering, "Dunarea de Jos" University of Galati, 47 Domneasca St., 800008 Galati, Romania

* Correspondence: florin.susac@ugal.ro

Abstract

Friction stir welding (FSW) began as a fairly specialized joining method, but over the past three decades it has evolved into something considerably more versatile, a manufacturing platform that now handles complex multi-material assemblies and solid-state additive processes with reasonable reliability. This review follows this evolution, paying particular attention to friction stir additive manufacturing (FSAM) and the persistent difficulties that arise when joining dissimilar systems: aluminum to steel or metals to polymers, where the fate of the joint is largely decided by how well the intermetallic compounds are kept under control. Machine learning, artificial intelligence, and high-fidelity numerical models are reducing the reliance on trial-and-error that once dominated parameter selection and defect prediction, bringing FSW closer to the operating principles of Industry 4.0. Hybrid variants, including ultrasonically assisted and underwater FSW, are also receiving attention here, as they offer researchers finer control over heat generation and plastic flow than the standard process allows. Throughout the study, microstructural observations are directly connected to mechanical results, with the aim of analyzing the current state of solid-state manufacturing and identifying the questions that most urgently need answering.

Keywords: friction stir welding (FSW); dissimilar joining; microstructural evolution; process optimization; hybrid welding

1. Introduction

1.1. Background and Industrial Context

Since its invention at the Welding Institute (TWI) in 1991, friction stir welding has emerged as one of the most important developments in solid-state joining [1]. The process, described in the seminal patents by Thomas et al. [1,3], operates by means of a profiled, non-consumable rotating tool that is inserted into the interface between two workpieces. No melting of the material occurs during the process; instead, friction between the spinning tool and the substrate generates localized heat, reducing the yield stress of the material until it reaches a highly plasticized state. The tool then advances along the joint line, mechanically extruding and forging the softened material behind the pin into a consolidated joint, one formed entirely below the melting point. Early investigations by Dawes and Thomas [2] confirmed that this solid-state approach was particularly well-suited for aluminum alloys, which tend to develop porosity and hot cracking when welded by conventional fusion methods.

The aerospace industry has played a significant role in transforming friction stir welding from a specialized procedure into mainstream manufacturing, as highlighted by Ahmed et al. [4] who note that the FSW process serves as a leading weight-reducing alternative to mechanical fastening in aviation. The basic process and its variants, including stationary shoulder and coil configurations, allow for the defect-free assembly of advanced aluminum and lithium-based structures. However,

 doi:10.20944/preprints202605.1246.v1

wider industrial adoption remains constrained by tool wear during high-temperature operations and the significant capital investment required for purpose-built multi-axis machines.

The marine industry has followed a similar trajectory to the aerospace industry. The assembly of large structural components, which must withstand persistent moisture exposure and cyclic mechanical loading, has led marine manufacturers to move towards optimized joining parameters and hybrid bolted and soldered configurations. Delzendehrooy et al. [5] have studied how these approaches address the long-term integrity requirements faced by marine assemblies. In the automotive sector, the shift to electric propulsion systems has significantly accelerated FSW innovation. Patel et al. [6] show that high-speed FSW is suitable for the production of lightweight battery trays on a large scale. The joining is performed at higher traverse speeds that limit the heat-affected zone (HAZ) in aluminum extrusions, preserving the hardness of the base metal and shortening cycle times without significantly degrading impact strength.

These cross-industry requirements continue to drive research in the field of aluminum joining, as noted by Dada et al. [7]. Dynamic thermal management and microstructural refinement have proven to be effective tools for limiting HAZ degradation in high-strength structural alloys, while real-time monitoring and adaptive control are increasingly seen as prerequisites for defect-free joining in complex disparate systems. However, Prabhakar et al. [8] acknowledge that there are still significant barriers to adapting friction stir welding (FSW) to a wider range of materials. Overcoming these requires reliable statistical optimization and continuous process monitoring to manage the variability inherent in thermomechanical processing. In the long term, expanding the industrial footprint of FSW will depend on the development of durable and cost-effective tools capable of withstanding extreme mechanical and thermal stresses while maintaining consistent joint quality, a challenge that has not yet been fully resolved.

1.2. Scope and Emerging Trends

Dissimilar material joining has become one of the most active areas of current FSW research, driven by the demand for components with spatially tailored mechanical properties that single-material designs simply cannot provide. Even joining dissimilar aluminum grades presents complications not encountered in single-material configurations. Cam et al. [9] point out that preventing brittle intermetallic phases at the interface and ensuring adequate material flow across it depend largely on tool placement, positioning of the harder alloy on the advancing side, and careful thermal management throughout the welding cycle. Kilic et al. [10] found that an inadequate ratio between rotation speed and traverse speed promotes volumetric defects, such as tunnel voids and bonding, either of which degrades tensile and fatigue strength in ways that are difficult to repair later.

Beyond aluminum–aluminum combinations, friction stir welding (FSW) has been gradually extended to more complex multi-material associations, and Shankar and co-workers [11] have shown that joining aluminum to non-aluminum metals is possible due to the solid-state nature of the process, that eliminates many of the incompatibilities associated with solidification and which make conventional fusion welding impractical for such combinations. Managing differences in thermal conductivity, expansion coefficient, and yield stress requires tight control over heat input and tool kinematics, with particular attention to limiting intermetallic growth. In the case of ferrous alloys, Khedr et al. [12] reviewed FSW applied to steels, noting that while this method successfully avoids solidification defects and brittle phase transformations, it imposes severe demands on tool design and durability. Shravan et al. [13] emphasize that thorough microstructural and mechanical testing is indispensable for establishing reliable correlations between process variables and structural performance.

Specific alloy classifications introduce their own processing constraints. Non-heat-treatable aluminum alloys, studied by Abnar et al. [14], respond to thermomechanical loading quite differently than heat-treatable ones, and achieving acceptable joint efficiency typically requires specialized tool geometries and some form of active cooling to limit grain growth and softening of the hot-melt zone (HAZ). Di Bella et al. [15] noted that the different configurations add an additional level of complexity

 doi:10.20944/preprints202605.1246.v1

and that process parameters must be carefully calibrated to account for the different flow stresses between aluminum grades, with adjustments to rotation speed, tool tilt, and material placement all necessary to ensure adequate mixing and prevent non-uniform thermal gradients.

Underlying all of this is the fundamental importance of thermal control, a theme that Khalafe et al. [16] repeatedly state that the balance between frictional heat input and subsequent cooling rate governs microstructural evolution, which in turn determines mechanical performance. Ambrosio et al. [17] provide the physical basis for this relationship, describing how surface heating from the tool shoulder and internal agitation from the pin together create the extrusion and forging conditions necessary to strengthen the joint and close residual voids. More recently, solid-state welding (FSW) has been extended to material classes that once seemed inaccessible. Sonar et al. [18] report on solid-state welding of high-entropy alloys (HEAs), showing that the process can preserve complex multicomponent microstructures without elemental segregation, a promising outcome for next-generation structural applications.

Engineering strategies originally developed to manage thermal softening in conventional aluminum alloys are adapted, with appropriate modifications, to the joining of increasingly harder materials. By completely eliminating the liquid-solid phase transition from the equation, FSW provides a thermomechanical framework flexible enough to accommodate both commercial alloys and advanced high-entropy systems, provided that the process parameters are chosen with sufficient care.

2. Advances in Dissimilar Material Joining

2.1. Aluminum-to-Steel Joining

The combination of aluminum alloys with steel in transportation applications is justified by the fact that steel provides structural rigidity and strength, aluminum reduces the mass of the structure, and a well-made joint between them provides both benefits simultaneously. The metallurgical reality, however, is considerably more complicated. The large differences in melting points and coefficients of thermal expansion between the two materials make conventional fusion welding practically impractical, and solid-state joining techniques have consequently become the main focus of research efforts in this field.

2.1.1. Process Mechanisms and Interfacial Characteristics

The intermetallic compound (IMC) layer that forms at the aluminum-steel interface is the product of both thermodynamic driving forces and kinetic diffusion processes, and its development follows a recognizable physical sequence. Yang et al. [19] proposed a conceptual model of this progression, one that begins with elemental interdiffusion, proceeds through localized nucleation, and culminates in the rapid and continuous growth of brittle intermetallic structures (see Figure 1). Thermodynamically, the phases that nucleate first are those with the lowest Gibbs free energy barriers under typical fusion welding (FSW) thermal conditions. Beygi et al. [20] showed that Fe_4Al_{13} and Fe_2Al_5 meet this criterion under standard FSW thermal cycles, preferentially precipitating at the interface before other phases have an opportunity to form (see Figure 2).

In a study on thermal fluid coupling in aluminum-steel lap joints, Geng et al. [21] demonstrated that the tool rotation speed simultaneously governs the maximum interface temperature and the material flow rate, a dual dependency that creates a narrow operating window. Too little heat input produces incomplete bonding defects, where the interface appears consolidated but lacks any significant metallurgical interaction, and too much heat leads to the formation of reaction layers thick enough to act as preferential crack initiation sites. The complexity of this operating window, where both insufficient and excessive heat input compromise joint integrity, underscores the need for predictive modeling approaches. Sekban et al. [22] addressed this challenge by developing an artificial neural network (ANN) trained on experimental data to model the formability of high-

 doi:10.20944/preprints202605.1246.v1

strength steel joints, allowing for the upfront optimization of process parameters and reducing the risk of cracking during post-weld forming.

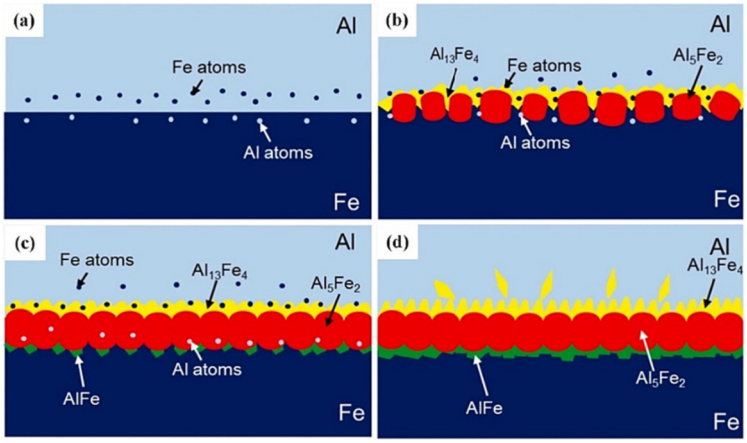

Figure 1. The mechanism of Fe–Al IMCs formation in different periods: (a) stage 1, (b) stage 2, (c) stage 3, (d) stage 4. [19].

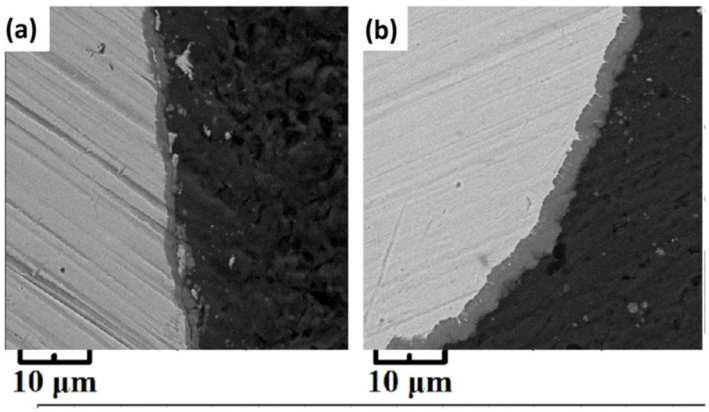

Figure 2. IMC layer at the interface of Al (AA5005)-St in butt joints made (a) underwater and (b) in air. Al is seen in the dark contrast, and St is seen in the white contrast. IMCs are observed as grey contrast. [20].

Taken together, these studies point to a consistent conclusion, namely, the mechanical integrity of dissimilar aluminum-steel joints is ultimately constrained by the Fe-Al intermetallic layer, and its control requires the simultaneous management of interfacial thermodynamics, plastic flow and thermal gradients. The introduction of specific alloying elements has emerged as a practical way to suppress the proliferation of brittle phases by modifying the local reaction thermodynamics. Meanwhile, thermomechanical simulations indicate that the architecture of the stir zone is shaped by frictional interactions at the tool-part interface, which means that the plastic flow must be carefully calibrated to avoid volumetric defects and ensure adequate interfacial bonding. Meeting the structural integrity standards demanded by industrial applications will likely require hybrid approaches that combine physical understanding of the underlying mechanisms with predictive tools, including finite element analysis and artificial intelligence, capable of predicting deformation behavior and formability limits under realistic loading conditions.

2.1.2. Strategies for Controlling Intermetallic Compounds (IMC)

Since the excessive growth of brittle IMC layers represents the main structural vulnerability in aluminum-steel joints, mitigation strategies have converged in two complementary directions: interface engineering and thermal management. In terms of tooling, pin geometry has proven to be

 doi:10.20944/preprints202605.1246.v1

a particularly effective variable. As shown in Figure 3, replacing a conventional cylindrical pin with a pin with circumferential grooves fundamentally alters the material flow pattern at the lapped interface. The modified geometry substantially increases in-plane plastic flow near the bond line, providing a mechanical stirring action that eliminates the stress-concentrating hook-like defects that would otherwise form at the interface and produces a planar bond free of stress concentrating morphological features [23].

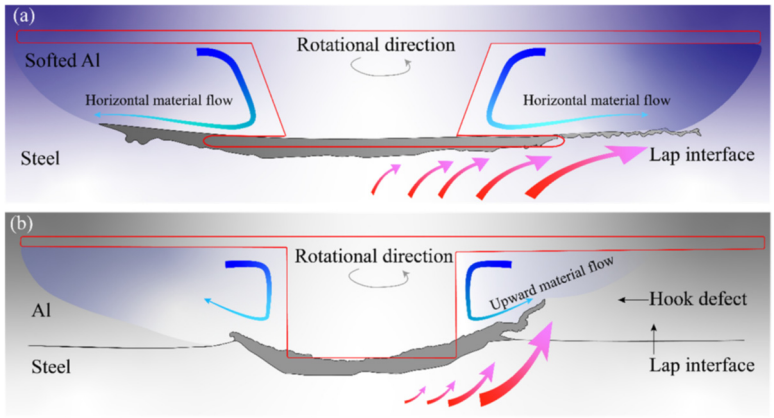

Figure 3. Interface formation mechanism. (a) Enlarged pin with circumferential notches. (b) Cylindrical pin. [23].

Parallel efforts have focused on the thermal conditions that determine the kinetics of IMC growth. Sahu et al. [24] coupled three-dimensional thermomechanical simulations with atomic-scale characterization to examine how frictional heat distribution patterns relate to IMC thickness. Their results indicate that controlling heat dissipation in the through-thickness direction sau controlling the directionality of heat dissipation across the joint thickness is the critical variable, restricting downward thermal diffusion reduces interfacial temperatures, thereby limiting the atomic diffusion kinetics responsible for excessive IMC growth, thereby limiting the atomic diffusion kinetics responsible for excessive IMC growth and preventing localized thickening of brittle phases that would otherwise serve as crack initiation sites.

The identity and behavior of the dominant intermetallic phases were examined in more detail by Geng et al. [25], who identified Fe_2Al_5 and $FeAl_3$ as the main phases in 5052-Al/DP590 steel joints. Their microstructural analysis revealed a a straightforward but concerning relationship sau a clear but detrimental relationship sau pur și simplu a direct and problematic relationship: increasing the tool rotation speed produces a produces a monotonic increase in interfacial heat input in the interfacial heat input, which in turn causes an approximately linear growth of the extremely brittle Fe_2Al_5 layer. Since fractures propagate predominantly through this specific phase, the authors argue that process parameters must be tightly controlled sau the process window must be narrowly defined to suppress the growth of the brittle Fe_2Al_5 layer.

2.1.3. Hybrid Approaches and Mechanical Performance

Conventional friction stir welding (FSW) sometimes is limited by the formation of thick, brittle intermetallic layers when joining metallurgically incompatible materials such as aluminum and steel, which has sparked interest in hybrid process variants, as highlighted by Liu et al. [26] who showed that superimposing ultrasonic vibrations on the FSW process significantly improves the quality of the joint. The high-frequency acoustic energy promotes the fragmentation of continuous IMC layers and leads to grain refinement. By reducing the flow stress of the material, ultrasound assistance widens the defect-free processing window and changes the failure mechanism from a mixed ductile-brittle mode to a purely ductile fracture, with a corresponding increase in the ultimate load capacity.

The introduction of a secondary heat source has been shown to be equally effective. Liu et al. [27] investigated a hybrid arc-FSW technique in which reducing flow stress and enhancing atomic

 doi:10.20944/preprints202605.1246.v1

diffusion at the interface, thereby promoting metallurgical bonding during the subsequent FSW pass. By depositing an initial intermediate aluminum layer using a bypass current MIG (BC-MIG) arc, the method restricts the brittle IMC layer to a thickness of less than 1.5 μm. As a result, tensile failure is redirected away from the vulnerable interface and toward the softer aluminum base metal. The hybrid arc-friction stir welding (AFSHW) process, illustrated in Figure 4, operates in two stages: an initial BC-MIG heat pretreatment to coat the galvanized steel surface, followed by substantial thermomechanical deformation by a multi-pass FSW tool. The approach illustrates the main advantage of hybrid systems: the use of sequential thermal and mechanical energy fields to design a resistant interface with minimal brittle phase formation.

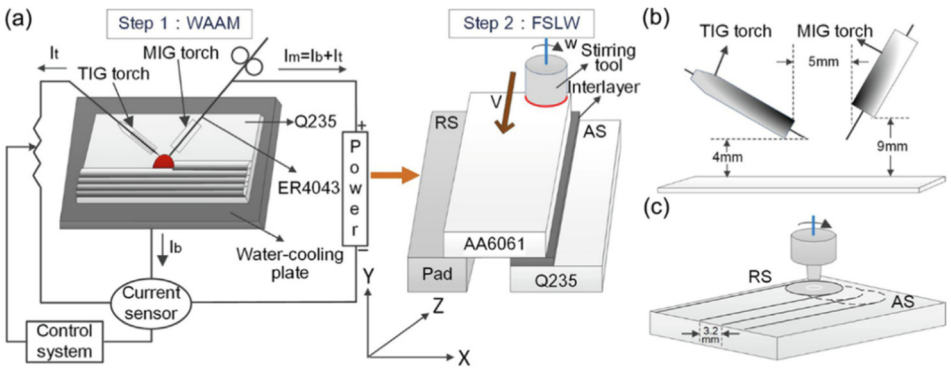

Figure 4. Schematic diagram of (a) the AFSHW process (step 1- SS, step 2-FSLW), (b) welding torch location in the step 1, (c) the position and relationship between adjacent pass in step 2 [27].

Pankaj et al. [28] observed that controlling the flow of immiscible materials is equally important for preventing internal defects and applied multiphase Computational Fluid Dynamics (CFD) to model the mixing behavior of aluminum and steel. Their simulations show the distribution of steel fragments in the aluminum matrix, a dispersion that strengthens the joint when uniform but triggers premature failure when the fragments agglomerate. The models show that insufficient rotation speeds generate insufficient material flow on the advancing side sau stagnant or poorly-mixed flow regions on the advancing side, while optimized heat inputs produce more uniform flow fields sau promote homogeneous material transport and suppress macroscopic voids. Coupling auxiliary energy sources with predictive fluid dynamics represents a significant step towards resolving the inherent incompatibilities of Al-steel systems.

2.1.4. Microstructural Evolution of the Steel Substrate

The mechanical integrity of a dissimilar joint depends not only on the interfacial bond but also on how the steel substrate responds to intense thermal cycling and severe plastic deformation. Ahmed et al. [29] examined mild steel for shipbuilding and found that thermomechanical processing causes substantial grain refinement, increasing local hardness. Their work shows that the traverse speed directly controls the cooling rate: higher speeds promote a refined bainitic microstructure that maximizes hardness, while lower speeds produce a softer matrix of polygonal ferrite and pearlite.

Advanced high-strength steels behave differently, as observed by Qiao et al. [30], who investigated the deformation mechanisms in twin-induced plasticity (TWIP) steel during FSW, finding that intense shear forces transform pre-existing annealing twins into regular high-angle grain boundaries, simultaneously causing the nucleation of nano-deformation twins. These microstructural changes govern the heterogeneous partitioning of plastic deformation across the weld in ways that are not easily predicted based on the properties of the base metal alone. In ultrahigh-strength quenching and partitioning (Q&P) steel, Wang et al. [31] documented a more complex phase evolution involving martensite and retained austenite. Rapid cooling in the stir zone produces fresh, untampered martensite and localized hardening, while the subcritical heat affected zone undergoes

 doi:10.20944/preprints202605.1246.v1

significant softening due to the decomposition of metastable retained austenite and subsequent precipitation of nanoscale carbides along the along prior austenite grain boundaries. As illustrated in Figure 5, this interplay between hardening and softening governs the overall stress distribution across the steel-aluminum joint. The decomposition of martensitic laths and retained austenite at subcritical temperatures triggers the precipitation of nano carbides and the formation of ultrafine ferrite grains with dense dislocation tangles, a microstructural configuration that provides strain hardening capability and helps protect against premature failure in the softened HAZ region.

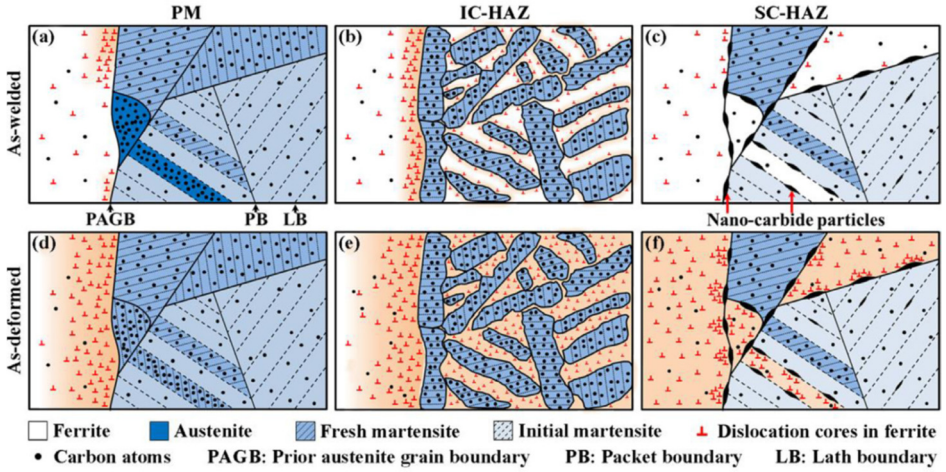

Figure 5. Schematic sketch drawings of the microstructural evolutions during welding and post-weld tensile deformation [31].

Deliberate control of thermomechanical cycling during friction stir welding (FSW) is important not only for the interfacial bond but also for tailoring the microstructure of the steel substrate as a whole, ensuring that localized phase transformations contribute to the mechanical performance of the joint rather than undermine it. Boumerzoug et al. [32] demonstrated how varying the traverse speed at a constant rotation rate directly affects the microstructural evolution and shear load in 6061-T6 aluminum welded to ultra-low carbon steel, while Dehghani et al. [33] determined that the joint strength in 3003-H18 aluminum and mild steel configurations is fundamentally related to the heat input and tool shoulder diameter. Among the process variables examined, tool offset emerges as a particularly influential variable sau tool offset proves critical, Zandsalimi et al. [34] found that an optimal offset during welding of 6061 aluminum to 430 stainless steel prevented void formation and generated a serrated interface characterized by robust mechanical interlocking.

Mitigating tool wear while maintaining joint strength has been another persistent research challenge, as studied by Watanabe et al. [35], who observed that shifting the tool offset toward the softer side of the aluminum effectively limited pin degradation while allowing the frictional action to remove the oxide layer from the steel surface. Zhang et al. [36] went further, protecting an H13 steel tool from direct contact with SUS304 stainless steel using a thickened aluminum interfacial plate. Meng et al. [37] proposed an friction stir lap welding with rivet reinforcement specifically designed to improve the load-bearing capacity of Al-steel assemblies through mechanical reinforcement. At the extreme end of thermal management, Li et al. [38] applied rotational speeds of up to 18,000 rpm to join 6061-T6 aluminum to 316L stainless steel, a pair also examined by Newishy et al. [39]. Under these specific conditions, the resulting intermetallic phases contributed to both mechanical bonding and improved corrosion resistance, a finding that warrants further investigation given the typically detrimental electrochemical role of IMC layers. The industrial scalability of such lap joints was demonstrated by Campanella et al. [40], who successfully integrated AA6016 aluminum with low-carbon steel for automotive body panels, demonstrating that tight parameter control can overcome the physical disparities and poor wetting behavior that complicates large-scale fabrication. Perhaps the most unexpected discovery in this area comes from Kasai et al. [41], who demonstrated that a

 doi:10.20944/preprints202605.1246.v1

controlled Fe-Al intermetallic layer can serve as a metallurgical bridge even for completely immiscible systems. The introduction of aluminum as an alloying element allowed the joining of steel and magnesium, with the Fe-Al intermetallic compensating for the fundamental lack of chemical affinity between iron and magnesium.

2.2. Aluminum-Magnesium Joining

Khalafe et al. [42] and Christy et al. [43] have analyzed in detail how parameter selection governs thermal distribution and weldability in Al-Mg systems. Thus, Khalafe summarizes that the optimal range for similar aluminum alloy joints is generally 600–1400 rpm, though dissimilar Al-Mg configurations may require narrower windows, and Christy confirms that exceeding the optimal rotation speed leads to grain growth, the formation of intermetallic phases by dynamic recrystallization, and a decrease in tensile strength. The common conclusion is that the parameter window for a defect-free joint is narrow and specifically dependent on the type and thickness of the material.

The combination of aluminum and magnesium alloys is of real interest for the design of lightweight structures in aerospace and automotive applications. The primary challenge arises from their high chemical affinity, which leads to the rapid precipitation of brittle intermetallic compounds, especially $Al_{12}Mg_{17}$ (γ-phase) and Al_3Mg_2 (β-phase), which can seriously compromise the integrity of the joint if thermal conditions are not strictly managed. A comprehensive scientometric analysis by Ahmed et al. [45] confirms that friction stir welding (FSW) outperforms conventional fusion methods for Al-Mg systems, but producing reliable joints requires rigorous control of the heat input to prevent eutectic reactions, which initiate at temperatures as low as 437 °C.

2.2.1. Material Flow and Mixing Behavior

The structural integrity of different Al-Mg joints depends largely on the dynamics of the material flow around the tool pin. Since aluminum and magnesium have distinct flow stresses and viscosities, their mixing behavior is inherently complex. Khaliq et al. [46] evaluated various butt-welding configurations and found that positioning the higher flow-stress material on the advancing side improves material transport and mechanical interlocking. The severe plastic deformation induced by this arrangement helps to fragment the continuous IMC layers, so that the joint strength comes to depend more on macromechanical interlocking than on purely metallurgical bonding. However, when mixing is inadequate, large continuous IMC networks remain intact along the boundaries of the stir zone, with adverse consequences on mechanical performance. A thermodynamic framework is therefore essential for interpreting these microstructural outcomes. Sen et al. [47] confirmed that Al_3Mg_2 and $Al_{12}Mg_{17}$ precipitate aggressively in the stir zone and severely compromise mechanical properties when thermal thresholds are exceeded. During severe plastic deformation, localized temperatures can easily exceed the eutectic point, triggering localized melting and brittle re-solidification, which is why maintaining processing temperatures below the solidus line is so important in practice. Nagaraja et al. [48] argue that friction stir welding (FSW) remains a promising route for aerospace Al-Mg structures, provided that flow-induced defects such as tunnel voids are managed through careful parameter optimization. By avoiding the solidification cracking associated with fusion welding, FSW retains a fundamental advantage for this material combination. Predictive modeling provides useful information on the internal dynamics of these joints, as noted by Yang et al. [49], who simulated material flow during different Al-Mg joints, identifying an asymmetric strain rate distribution. The offset of the tool towards the magnesium side modulates the volume of mixed material and limits the macroscopic accumulation of brittle phases. Using a CFD model with a shear boundary coupled with thermo-mechanical flow, the authors quantitatively mapped the three-dimensional mass transfer. Their results show that although most of the plasticized material follows a relatively straight trajectory, a portion of the magnesium on the advancing side becomes trapped in what they describe as a chaotic vortex, a maelstrom flow that forces the material downward through multiple concentric revolutions around the pin, as illustrated in Figure 6. This mechanism

 doi:10.20944/preprints202605.1246.v1

explains why magnesium accumulates consistently at the root of the weld, while aluminum dominates the upper regions of the agitation zone. This distribution pattern suggests that brittle phase clusters are most likely to concentrate at the weld root, where magnesium accumulation is greatest, making this region the critical site for crack initiation.

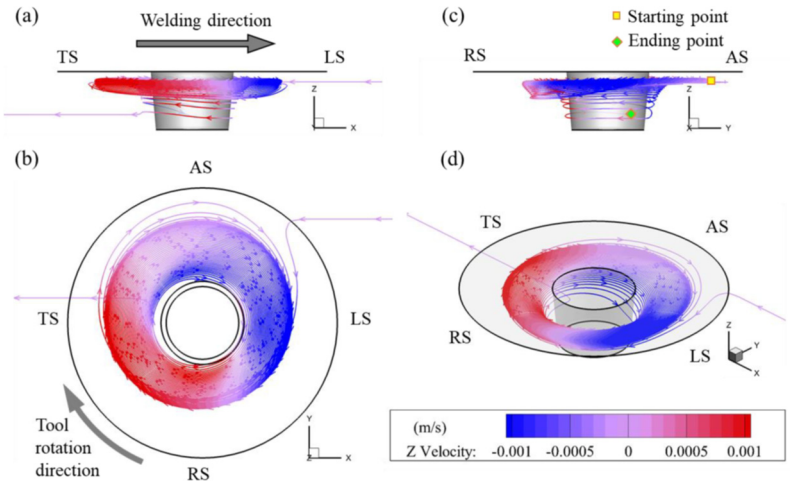

Figure 6. A typical path of maelstrom flow initiated from Y = 5 mm Z = 0.5 mm and Z-direction velocity along the path, predicted by the shear boundary model. (a) RS view. (b) Top view. (c) LS view. (d) Top-RS–LS view [49].

2.2.2. Interface Enhancement Techniques

Given the inherent brittleness of Al-Mg intermetallic, recent work has increasingly focused on interface design to modify the fundamental bonding mechanisms. Zhao et al. [50] investigated ultrasonic vibration-assisted FSW, finding that high-frequency acoustic energy breaks continuous IMC layers into discrete dispersed particles, disrupting crack propagation paths and improving joint ductility. Their near-in-situ microstructural analysis showed that acoustic softening reduces the flow stress of the material, promoting increased plastic flow and redistributing the magnesium-rich material toward the retreating side and limiting the kinetic conditions favorable for IMC growth by disrupting the continuity of the reaction interface.

The introduction of third-body materials presents another viable strategy, as pointed out by Abdollahzadeh et al. [51] who incorporated a zinc interlayer alongside TiC nanoparticles, the zinc foil acting as a localized diffusion barrier promoting the formation of more favorable Mg-Zn and Mg-Al-Zn compounds at the expense of the brittle Al-Mg intermetallics. The uniformly dispersed TiC nanoparticles provided additional microstructural reinforcement, pinning the grain boundaries and further limiting the growth of the IMC. The uniformly dispersed TiC nanoparticles provided additional microstructural reinforcement by simultaneously pinning grain boundaries and acting as heterogeneous nucleation sites, promoting significant grain refinement throughout the stir zone.

Beyond chemical and acoustic interventions, Xu et al. [52] demonstrated that modifying the macroscopic geometry of the joint by introducing an interface with multiple interconnected grooves represents another practical route for structural improvement, specifically designed to restrict the effective contact area between the aluminum and magnesium plates. As shown in Figure 7, the serrated profile improves mechanical interlocking while deliberately reducing the metallurgical reaction zone. By relocating the metallurgical reaction zones away from the thermal center of the tool, the design suppresses the diffusion kinetics responsible for excessive IMC proliferation. Xu et al. reported that this design increased the load-bearing capacity by more than threefold compared to standard butt-welding configurations.

 doi:10.20944/preprints202605.1246.v1

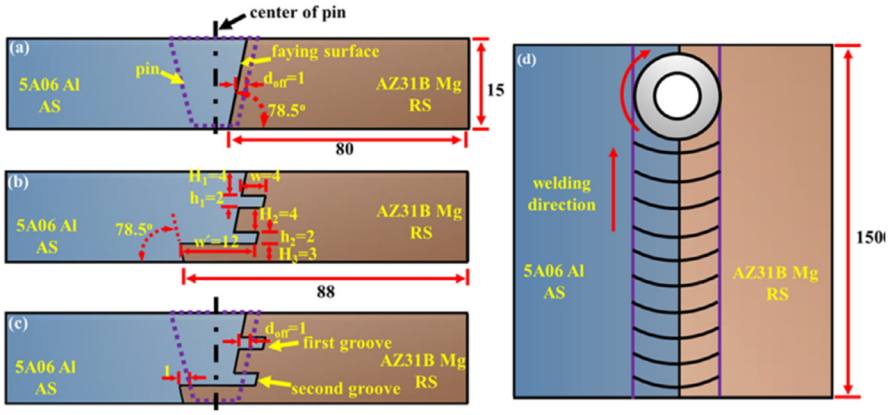

Figure 7. Schematic illustration of different joint configuration: (a) conventional joint; (b, c) innovative joint; (d) Al/Mg FSW process [52].

2.2.3. Influence of Tool Design and Process Variants on Joint Quality

Ke et al. [53] analyzed double-sided friction stir spot welding (FSSW) of magnesium alloys, demonstrating that tool geometry and process variant selection govern the thermal cycle and, consequently, the quality of the resulting joint. Using a coaxial tool system with independently controlled pins, as illustrated in Figure 8, the approach allows for simultaneous symmetrical penetration from both the top and bottom surfaces. This configuration promotes a more uniform thermal distribution across the sheet thickness and directs the material flow towards the midplane, effectively closing the keyhole defect left behind by conventional FSSW and producing a homogeneous stir zone microstructure.

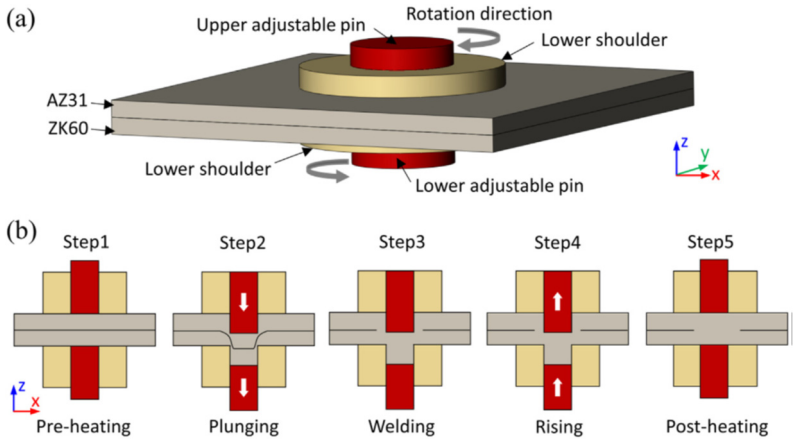

Figure 8. (a) Diagram of the Flat DSAT FSSW system; (b) Schematic sketch of the welding process [53].

Electrically assisted variants are attracting increasing interest for similar reasons, with Xiaoqing et al. [54] demonstrating that pulsed current applied during FSW for dissimilar Al-Mg joints induces an electro-plastic effect that reduces the flow stress of both materials, facilitating adequate mixing at lower temperatures and mechanical loads facilitating adequate mixing at lower temperatures and mechanical loads, thereby restricting the excessive growth of intermetallic compounds. The application of a pulsed current effectively widens the processing window, allowing defect-free joints under conditions that would otherwise lead to failure, and shifts the fracture mechanism from brittle interfacial cleavage to a more ductile mode.

Establishing a rigorous correlation between process parameters and mechanical outcomes remains essential. Using Response Surface Methodology (RSM), Solomon et al. [55] mapped the interactions between rotation speed, traverse speed, and tool tilt angle for magnesium alloys, identifying the optimal parameter windows to maximize tensile strength without extensive empirical

 doi:10.20944/preprints202605.1246.v1

iteration or without systematic experimental campaigns. The initial condition of the base material is equally important. Xu et al. [56] showed that prior microstructural refinement of AZ61 magnesium, achieved by a high-load, low-speed FSW strategy, substantially improves the alloy's superplasticity and subsequent weldability. The intense plastic deformation at lower heat inputs causes a fine, equiaxed grain structure that improves both ductility and load-bearing capacity. The shift toward advanced tool configurations and hybrid processes reflects a broader research effort to address the inherent weldability challenges of lightweight alloys in the aerospace and automotive sectors. Although FSW successfully circumvents the severe solidification defects of fusion welding [57], the thermodynamic tendency of aluminum and magnesium to form brittle intermetallic, especially $Al_{12}Mg_{17}$ and Al_3Mg_2, remains the main barrier to joint integrity [58]. Controlling these continuous brittle networks requires precise microstructural management. For lap joints between AZ31B Mg and AA6061-T6 Al, Bandi and Bakshi [59] showed that to restrict the thickness of the IMC layer and suppress eutectic formation and maintain the lapped shear strength.

In order to disrupt the formation of IMCs, Lv et al. [60] demonstrated that ultrasonically enhanced FSW modifies the local thermal profile and widens the material flow path and widens the material flow path, improving macroscopic mechanical interlocking, a strategy that researchers are increasingly turning to precisely because of these combined effects. Building on this, Liu et al. [61] applied ultrasonically assisted stationary shoulder FSW to physically break up continuous IMC layers into discrete particles - a structural change that disrupts continuous crack propagation paths and significantly improves the tensile properties of Al-Mg joints.

The microstructural evolution in the agitation zone also determines how the weld holds up in service, with Jayaraj et al. [62] demonstrating that intense mechanical mixing of Al and Mg, combined with IMC precipitation, generates localized galvanic microcells that degrade corrosion resistance. Mitigating these vulnerabilities requires strict thermal control to minimize the IMC volume fraction [63], with Fu et al. [64] experimentally defining this operational window and demonstrating that a moderate rotation rate of 600–800 rpm, combined with a low traverse speed and tool offset towards the magnesium side, reaches up to 70% of the tensile strength of the aluminum base metal sau of the weaker base metal. To map these thermomechanical interactions without relying entirely on physical testing, Baruah et al. [65] used three-dimensional finite element modeling to simulate friction stir spot welding of Al-6061 and Mg-AZ31B, clarifying the stress and temperature distributions governing the bond, reflecting the increasing focus of the field on computational modeling. Complementing this approach, Efa et al. [66] combined RSM with Artificial Neural Networks, extending the predictive capability beyond single-response optimization to multi-objective parameter selection. Together, these modeling and optimization tools are progressively reducing the experimental burden of process development for dissimilar Al-Mg systems.

2.3. Aluminum-Copper Joining

The joining of aluminum with copper is a well-established requirement in the electrical and power generation sectors. This combination leverages the excellent electrical and thermal conductivity of copper, along with the low weight and cost of aluminum, making it a standard choice for busbars, battery terminals, and heat exchangers. However, as with most dissimilar metal systems, the precipitation of brittle intermetallic compounds poses a persistent challenge to long-term mechanical and electrical reliability.

2.3.1. Electrical and Thermal Performance Considerations

Sun et al. [67] reviewed the current landscape of Al-Cu friction stir welding, noting that while solid-state processing effectively circumvents the high electrical resistance caused by fusion welding defects, management of the IMC layer thickness remains essential. A thin and continuous IMC layer facilitates bonding, while excessive growth sharply increases the electrical resistance and induces embrittlement of the joint.

 doi:10.20944/preprints202605.1246.v1

To address these performance limitations, Bagheri et al. [68] used friction stir spot welding (FSSW) to create Al/SiC/Cu composites, demonstrating that the addition of SiC nanoparticles increases the contact surface hardness and wear resistance without severely degrading the electrical conductivity. Extending this approach sau In a related investigation, Bagheri et al. [69] examined the addition of nanoparticles in pure AA2024/Cu joints, finding that the nanoparticles exert a pinning effect that refines the interfacial grain structure and homogenizes the electrical properties across the weld. As shown in the Energy Dispersive Spectroscopy line scans in Figure 9, SiC additions result in a slightly thicker IMC layer, 3.1 μm compared to the conventional 1.9 μm, due to increased frictional heat and material agitation. It is important to note, however, that this extended reaction zone remains free of microcracks, suggesting that even with a higher volume of brittle phases such as Al_2Cu and Al_4Cu_9, structural integrity and conductive path stability are preserved by a mechanically sound interface with preserved diffusion bonding characteristics.

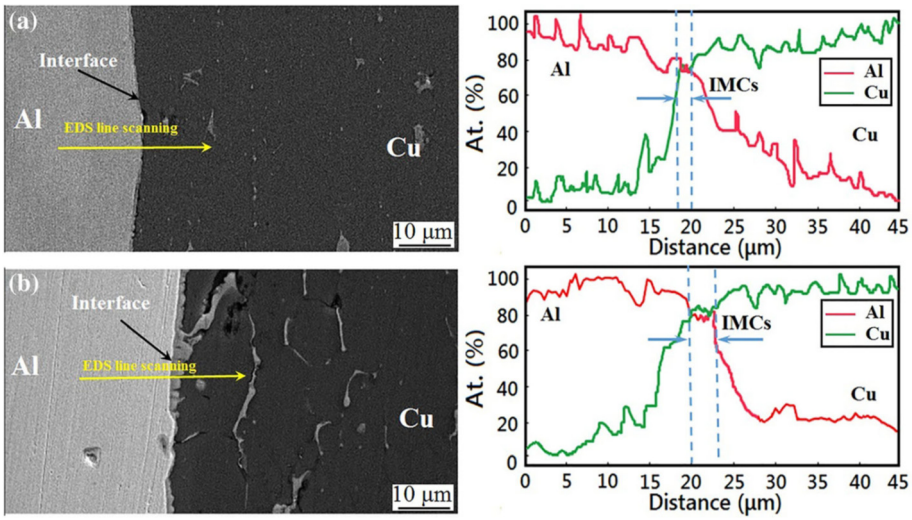

Figure 9. The thickness of an intermetallic compound layer formed at the aluminum–copper interface during (a) conventional FSSW and (b) FSSW with SiC nanoparticles [69].

Incorporating reinforcing nanoparticles into the Al-Cu boundary thus offers a dual benefit, it strengthens the joint against wear through particle-induced hardness enhancement and grain boundary pinning, while simultaneously generating the refined, defect-free microstructure required to maintain stable electrical and thermal connections.

2.3.2. Microstructural Evolution and Tuning of the IMC Layer

With the microstructural development at the Al-Cu interface being driven by severe plastic deformation and tool-induced frictional heating, Ji et al. [70] introduced a “double friction-stirring” approach in which the coupling of mechanical interlocking with a precisely controlled diffusion layer substantially increases the load-bearing capacity of the joint compared to standard FSSW. The deformation of the copper rivet creates a double anchoring effect, a copper anchor at the top surface and an aluminum anchor at the joint interface, that eliminates kissing defects and ensures a strong metallurgical bond.

Auxiliary acoustic energy has proven to be a reliable tool for controlling microstructural evolution, with You et al. [71] demonstrating that integrating ultrasonic vibrations into a stationary shoulder FSW configuration causes the acoustic field to break continuous IMC layers into isolated particles, halting crack propagation through brittle phases and improving joint ductility. Figure 10 illustrates this interfacial evolution, initial severe plastic deformation fragments and redistributes the parent phase constituents, after which superimposed high-frequency stress waves concentrate cyclic stresses at the brittle IMC interfaces, inducing fracture and fragmentation of the continuous layers

 doi:10.20944/preprints202605.1246.v1

that breaks the crack-sensitive IMC layers into fine particles and interrupts potential fracture pathways.

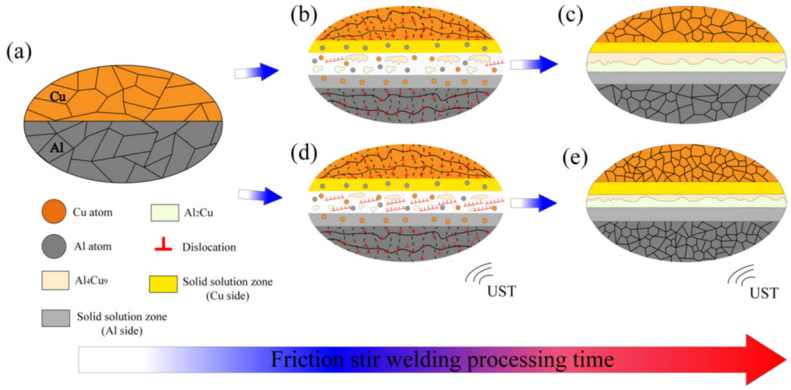

Figure 10. Schematic diagram for the interfacial microstructure evolution during the welding process: (a) pre-welding state, (b) DSSFSW intermediate state, (c) DSSFSW final state, (d) U-DSSFSW intermediate state, (e) U-DSSFSW final state [71].

Restricting heat input is another key control strategy, with Zhao et al. [72] demonstrating that the use of a stationary shoulder tool suppresses the thermal gradient along the weld. By eliminating shoulder rotation, frictional heat is significantly reduced, narrowing the heat affected zone and preventing the growth of harmful Al_2Cu and Al_4Cu_9 layers. Experimental measurements confirm that this technique reduces the IMC layer thickness from 2.4 μm in conventional FSW to approximately 1.6 μm, maintaining the IMC layer below the threshold thickness associated with significant embrittlement. Managing IMCs becomes even more complex in submerged conditions, with Mao et al. [73] demonstrating that the rapid cooling inherent in an aquatic environment severely restricts atomic diffusion in submerged FSW of Al-Cu plates, resulting in a thinner and more uniform IMC layer dominated by phases with comparatively lower brittleness, such as $CuAl_2$.

Producing reliable and diverse Al-Cu joints ultimately requires a comprehensive approach. By combining mechanical interlocking strategies such as friction-stir riveting, auxiliary acoustic energy, and strict thermal management through stationary shoulders or active cooling, engineers can confine the brittle intermetallic to a dispersed, discontinuous morphology that preserves both structural and electrical integrity.

2.3.3. Role of Interlayers and Process Parameters

The introduction of interlayers offers a practical way to manage interfacial reactions in dissimilar welds, with Abdollahzadeh et al. [74] demonstrating both through simulation and experiment that a zinc interlayer acts as a physical buffer in Al-Cu joints, preventing direct contact between the base metals and modifying the thermodynamic driving forces responsible for IMC formation, ultimately resulting in a more ductile interface. Their finite element analysis revealed a critical trade-off: while larger shoulder diameters increase frictional heat and improve material plasticity, they simultaneously reduce the uniformity of stress distribution in the weld zone, requiring a careful balance between thermal generation and mechanical stability.

Since mixing efficiency is directly related to tool geometry, He et al. [75] found that the threaded stud design significantly improved vertical mixing, a downward flow essential for fracturing oxide films and dispersing reaction products, helping to prevent the formation of continuous brittle networks. Their simulations specifically showed that the combination of threaded and flat features generated a high-velocity downward material trajectory, which eliminated the weak bond defects typically observed at the root of the stir zone. The strength of the joint can be further improved by deliberately influencing the IMC phases that precipitate during welding, with Beygi et al. [76] identifying a mechanism whereby intermittent θ-phase intermetallic act as crack arresters, a

 doi:10.20944/preprints202605.1246.v1

discontinuous reaction layer preventing catastrophic cleavage and forcing propagating cracks to bypass the harder parent materials.

Beyond tool design, Bagheri et al. [77] established a clear empirical link between dwell time and shear strength in Al/SiC/Cu spot welds, with microstructural evaluations confirming that shorter dwell times limit grain growth in the stir zone and produce superior shear strength according to the Hall-Petch relationship, with parameters such as rotation speed and dwell time thus directly controlling the heat input. Vaneghi et al. [78], exploring pinless FSW, observed that pin removal reduces mechanical stir, requiring extremely precise control over the shoulder plunge depth to maintain adequate bonding pressure. Their work also showed that although an intermediate zinc layer aids bonding, prolonged dwell times introduce excessive heat that causes the proliferation of the brittle Al_2Cu phase, ultimately compromising the integrity of the joint.

Different alloy combinations require customized analytical approaches. For AA5083-Cu joints, Bagheri et al. [79] showed that the optimal processing window for joining non-heat-treatable aluminum to copper differs significantly from the heat-treatable variants. Their macrographic analysis revealed a distinct "copper ring" on the advancing side, formed as the copper is extruded into the aluminum matrix, a structure that provides robust macroscopic interlocking, compensating for the limited atomic diffusion at lower processing temperatures. Therefore, thermodynamic modification through interlayer additions sau chemical barrier effect of interlayers to ensure that mechanical and metallurgical bonds work together to suppress brittle failure [80]. To mitigate uneven mixing and excessive heat, Bora et al. [81] demonstrated through Analysis of Variance that strategic offset of the tool from the joint line governs material flow and thermomechanical mixing, leading to substantial gains in load-bearing capacity, with spatial parameters such as tool offset being precisely tuned by researchers for this purpose. By embedding thermocouples in AA7075-T6/pure copper joint specimens, Çakan et al. [82] mapped the direct correlation between rotational speeds in the range of 660–1500 rpm and peak temperatures, reinforcing the need for strict thermal management. Wei et al. [83] investigated the influence of tool material and geometry, process parameters, plate overlap sequence, and the use of a heat sink on the quality of Al–Cu joints made by Friction Stir Welding (FSW), aiming to obtain defect-free joints with improved mechanical properties. Specialized FSSW variants have been developed for lap joint configurations, with Devarajan et al. [84] identifying tool penetration rate, rotational speed, and dwell time as the main determinants of mechanical interlocking and electrical conductivity in such Al–Cu joints. Since conventional FSSW inevitably leaves a residual keyhole defect, Gao et al. [85] proposed a modified friction-stirring technique combined with an intermediate zinc layer. This modified approach effectively fills the keyhole, increasing the joint strength by 40%, while the zinc buffer suppresses the formation of brittle Al_2Cu and Al_4Cu_9 phases, promoting instead the precipitation of ductile lamellar eutectics and Zn-rich $CuZn_5$ compounds, preserving structural integrity.

2.4. Metal-to-Polymer and Composite Joining

The demand for extreme lightness and corrosion resistance in aerospace and automotive applications has generated considerable interest in metal-polymer hybrid structures. Joining metals to thermoplastics, however, is a fundamentally different problem from metal-metal joining; the severe disparities in melting temperatures and the complete lack of chemical affinity between the two classes of materials preclude most conventional approaches. As presented by Barakat et al. [86], FSW offers a practical solid-state solution, with the metal being plasticized and mechanically pressed into the polymer, the integrity of the joint relying on macroscopic and microscopic interlocking rather than chemical bonds. Rudrapati [87] notes that excessive heat input readily degrades the polymer matrix or fractures the reinforcing fibers, dramatically reducing joint efficiency, meaning that the operational window for metal-polymer systems is considerably narrower than for metal-metal configurations.

The strength of the joint in these hybrid systems is dictated almost entirely by the quality of the interface. Wang et al. [88], investigating the friction stir lap welding of light metals onto carbon fiber

 doi:10.20944/preprints202605.1246.v1

reinforced polymer (CFRP) composites, demonstrated that the deliberate induction of a hook-like penetration of the plasticized metal into the polymer improves mechanical anchoring, provided that thermal degradation is avoided. To maximize this effect, they introduced a laser ablation pretreatment to establish a multi-scale bonding mechanism. As illustrated in Figure 11, the interface is strengthened at four levels: macro-mechanical interlocking driven by tool pressure, micro-mechanical anchoring in laser-ablated grooves, nano-mechanical clamping within surface pores, and the formation of C–O–Al chemical bonds. Laser-induced texturing expands the contact area, allowing the molten polymer to penetrate the metal substrate while facilitating atomic-level reactions between the PA66 matrix and the Al_2O_3 surface oxide.

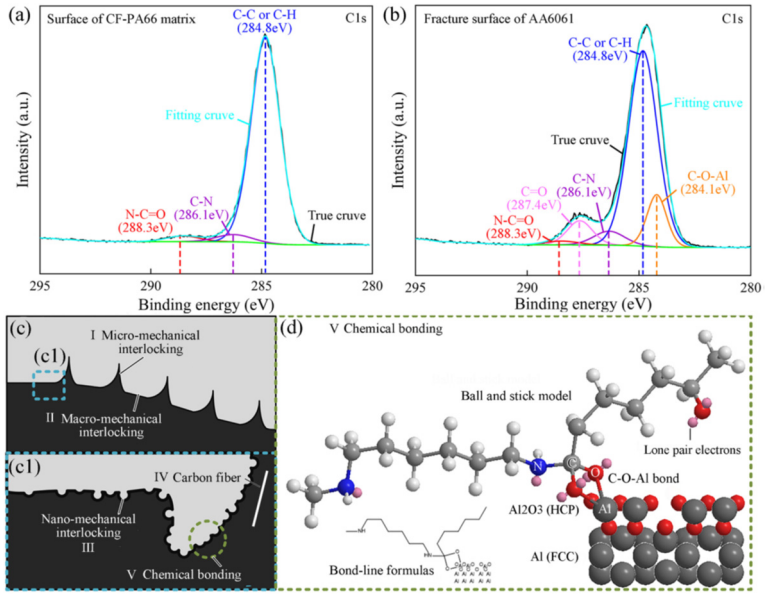

Figure 11. XPS analysis and interface enhancement mechanism of hybrid joints: (a) XPS analysis of as-received CF-PA66 matrix; (b) XPS analysis of residues on AA6061 side after joint fracture; (c) interface enhancing effect including macro/micro/nano-mechanical interlocking and chemical bonding; (d) the ball and stick model along with bond-line formulas revealing the chemical bonding between PA66 matrix and Al2O3 [88].

Driven by the need for improved material transport, Nian et al. [89] introduced a multi-vortex sealing flow lap welding technique that induces complex flow patterns, forcing the polymer into surface irregularities on the metal and thereby establishing a robust three-dimensional interlocking network that significantly increases shear strength. As illustrated in Figure 12, while a standard tapered pin generates a defect-prone upward-directed flow, the proposed multi-stage pin geometry creates localized vortex-like circulation at each level. These flow dynamics effectively trap the rising polymer, sealing it within the joint and accelerating mixing to produce a dense, defect-free interlocking zone.

The trajectory of metal-polymer bonding research reflects a clear shift away from relying entirely on macroscopic deformation, towards deliberate interfacial engineering through multi-scale surface texturing and advanced tool geometries designed to provide mechanochemical synergy.

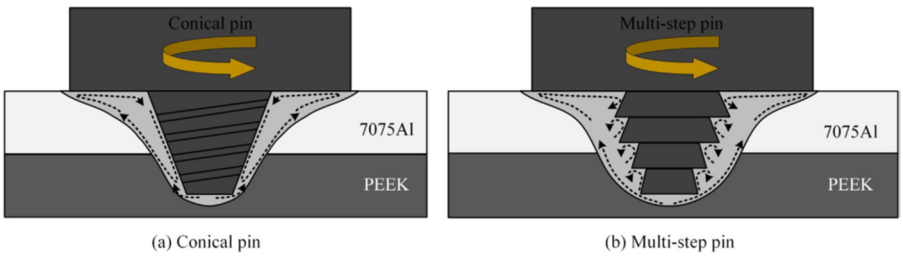

Figure 12. Schematic diagrams of material flow behaviors under different pins [89].

 doi:10.20944/preprints202605.1246.v1

2.4.1. Friction Stir Welding of 3D Printed Polymers

A more recent application of FSW addresses the assembly of additively manufactured polymer sheets, highlighted by Vidakis et al. [90] who optimized process parameters for 3D printed acrylonitrile butadiene styrene (ABS), showing that FSW can successfully join or repair printed parts while maintaining mechanical properties comparable to those of conventionally processed material. Their work in the context of hybrid additive manufacturing emphasizes that tight control over tool geometry and tilt angle is essential to tune the thermal field and avoid severe material degradation.

In a related study on 3D printed polylactic acid (PLA), Vidakis et al. [91] used a full factorial design to determine that rotational speed is the dominant factor in suppressing defects such as flash formation and voids in biodegradable polymers. Figure 13 provides a comparative microstructural analysis of the resulting welds. The micrographs clearly show the morphological differences between a solid joint, marked by a continuous agitation zone and a clear onion-ring pattern of mixing, and a defective joint containing macroscopic voids and tunnel defects. These findings reinforce the principle that structural integrity in thermoplastic FSW depends on maintaining temperatures within a tightly restricted window, hot enough to allow plastic flow, but cool enough to prevent thermal degradation.

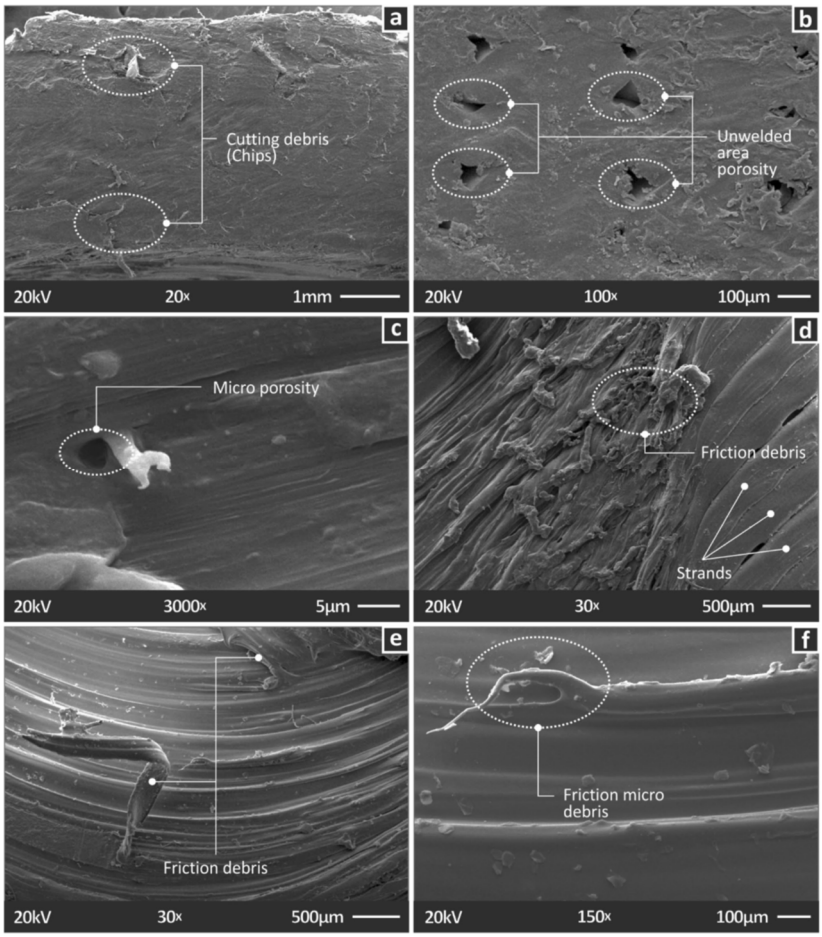

Figure 13. SEM images of the preliminary study specimen: a Side surface at the HAZ area, in 20 X. magnification, b side surface of the specimen on the left side of the HAZ, in 100 X. magnification, c side surface of the specimen on the right side of the HAZ, in 3000 X. magnification, d top view of the specimen on the right side of the HAZ, in 30 X magnification, e top view of the specimen at the center of the HAZ, in 30 X. magnification, and f top view of the specimen at the center of the HAZ, in 150 X magnification [91].

 doi:10.20944/preprints202605.1246.v1

Together, these studies validate hybrid additive manufacturing as a practical industrial approach, demonstrating that solid-state welding can circumvent the dimensional limitations inherent in 3D printing and enable the fabrication of large, structurally robust polymer assemblies.

2.4.2. Tool Design and Surface Pretreatment

Khalaf et al. [92] examined the thermomechanical behavior of high-density polyethylene during FSW using various pin profiles, finding that threaded cylindrical pins significantly improved vertical mixing and heat generation, both of which are necessary for semi-crystalline polymers to reach the correct viscoplastic state. Their CFD models showed that threaded pins reached a peak temperature of 158 °C, higher than that recorded for square or triangular alternatives, establishing a balance between shear stress and frictional heat that avoids both poor consolidation and material degradation. The flow field induced by the threads forces the molten polymer downward, promoting a uniform viscosity distribution in the agitation zone, while polygonal pins tend to generate a pulsating, turbulent flow that frequently introduces internal voids. For more demanding applications, where mechanical interlocking alone is often insufficient, Wang et al. [93] developed a physicochemical surface pretreatment that modifies the surface energy of the metal prior to welding. This approach generates a hybrid joint based simultaneously on chemical adhesion and mechanical anchoring, thereby doubling the load-bearing capacity compared to untreated specimens. As shown in Figure 14, the method creates macroscopic grooves to facilitate resin flow and physical interlocking, while silane molecules are grafted onto the newly micro-roughened surface. The silane functions as a molecular bridge, promoting the formation of interfacial Al-O-Si-C covalent bonds that work in tandem with macroscopic mechanical anchors to resist joint failure.

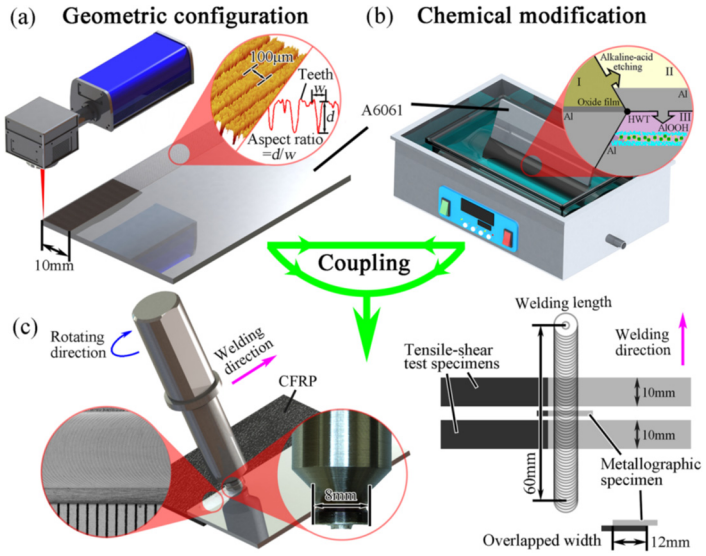

Figure 14. Schematic illustration of surface pretreatment and FSLW process [93].

Further development of hybrid metal-polymer joining depends on a comprehensive manufacturing strategy that synchronizes optimized tool kinematics with advanced surface engineering, enabling multi-scale bonding mechanisms that overcome the deep physical and chemical incompatibilities of the base materials.

2.5. Joining High-Entropy and Specialty Alloys

Friction stir welding (FSW) is increasingly applied to advanced materials, including high-entropy alloys (HEAs) and superalloys, which are notoriously difficult to process by conventional fusion welding due to severe elemental segregation and susceptibility to cracking. Do et al. [94] successfully joined a CoCrFeMnNi high-entropy alloy (HEA) to STS304 stainless steel, observing that

 doi:10.20944/preprints202605.1246.v1

the solid-state nature of FSW suppressed the formation of deleterious sigma phases and maintained a simple face-centered cubic (FCC) structure at the interface. Subsequent mechanical testing showed that these dissimilar joints exhibit exceptional properties: the HEA side fractured in a ductile manner, while the stainless-steel side failed in a mixed ductile-brittle manner, indicating that joint quality is comparable to, or exceeds, that of the base metals themselves. Similarly, Hu et al. [95] examined the recrystallization behavior of a medium-entropy CoCrNi alloy, finding that the severe plastic deformation inherent in FSW triggers substantial grain refinement through dynamic recrystallization, with a corresponding increase in material strength. The grain orientation distribution (GOS) maps provided in Figure 15 illustrate this clearly: recrystallized grains, shown in blue, dominate the microstructure of the agitation zone due to the high heat input, while deformed grains, shown in red, are relatively rare, confirming dynamic recrystallization as the dominant restoration mechanism driving grain refinement.

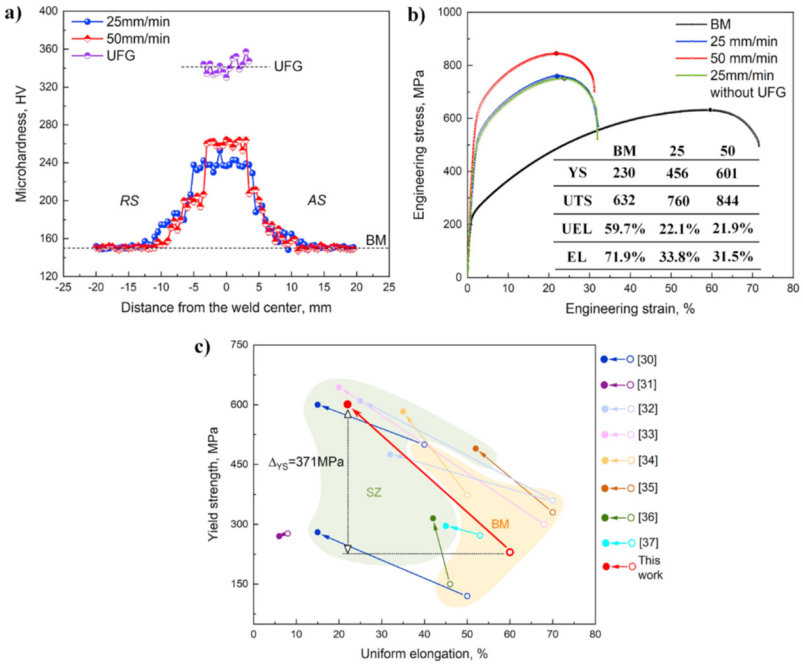

Figure 15. a) Microhardness distributions, b) engineering stress-strain curves, c) comparison of YS versus UEL of various HEAs and this work before and after FSW [30–37]. YS: yield strength, UTS: ultimate tensile strength, UEL: uniform elongation, EL: elongation [95].

Significant progress has also been made in highly corrosive environments, with Cao et al. [96] demonstrating that submerged FSW applied to super duplex stainless steel, through rapid cooling provided by the aqueous medium, produces an ultrafine-grained microstructure and a well-balanced austenite-ferrite ratio. The result was a simultaneous improvement in both strength and ductility, a combination notoriously difficult to achieve in duplex steels. Crucially, the submerged process prevented the elemental partitioning that typically accompanies fusion welding, resulting in pitting corrosion resistance comparable to that of the base metal. In a study focused on low-temperature processing, Su et al. [97] analyzed the cooling rates of welds in titanium alloy TA5, concluding that tight control of the β-to-α phase transformation is essential to prevent embrittlement in titanium friction stir joints.

3. Hybrid and Derivative Variants of the FSW Process

The development of new hybrid and derivative techniques of the FSW welding process, designed to address specific metallurgical constraints, has emerged as a response to the limitations

 doi:10.20944/preprints202605.1246.v1

of conventional techniques regarding: excessive heat generation, grain coarsening, and the accumulation of residual stresses.

3.1. Underwater Friction Stir Welding (UFSW)

Underwater friction stir welding (UFSW) has proven to be a highly effective hybrid method, used for heat-sensitive materials.

Optimizing UFSW parameters requires distinct strategies compared to conventional processing, so Madani et al. [99] applied Taguchi and ANOVA methods to optimize process parameters for welding AA2017 aluminum alloy. They found that the tool rotation speed is the parameter with the greatest influence on joint quality.

To generate sufficient plasticity, high tool rotation speeds are required to compensate for the cooling effect of the water and prevent the occurrence of "wormhole" defects or those caused by incomplete fusion. Using response surface methodology, researchers determined that, although feed rate affects productivity, the rotational speed must be calibrated to be around 1400 rpm. This maximizes tensile strength without introducing excessive heat that would lead to the dissolution of the alloy's hardening precipitates.

Sabry et al. [100] studied Al-Mg-Si T-joints using both conventional FSW and UFSW, observing that the underwater environment effectively suppressed grain growth in the stir zone, resulting in a significantly finer microstructure. This is evident in the comparative SEM images in Figure 16, where both welding methods refine the elongated grains of the base metal, yet the UFSW specimen exhibits significantly finer and more uniformly distributed equiaxed grains and secondary phase particles — a direct consequence of the rapid heat absorption by the aqueous environment, which effectively preserves the recrystallized structure and severely limits the time available for grain growth. A potential concern is that penetration depth must be carefully controlled, as rapid cooling can cause excessive hardening at the weld root, which acts as a stress concentrator if the material is not adequately plasticized.

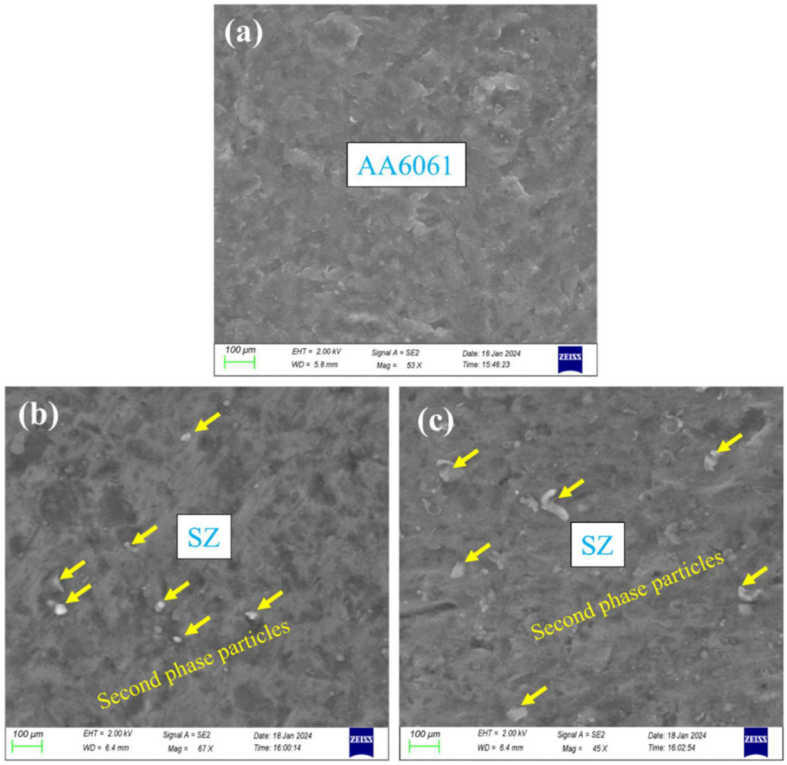

Figure 16. SEM images of welded samples showing second phase particles (a) base metal (BM), (b) SZ of FSW (1800 rpm, 7 mm) and (c) SZ of UFSW (1800 rpm, 7 mm) [100].

 doi:10.20944/preprints202605.1246.v1

Saravanakumar et al. [102] demonstrated that different tool profiles, conical, cylindrical and hexagonal, interact in quite different ways with the underwater environment. Since the plasticized material solidifies rapidly underwater, a tool profile that strongly favors vertical flow of the material is essential to ensure adequate mixing before the material actually solidifies. As shown in Figure 17, the straight hexagonal profile creates a pulsating stirring action that is quite different from the constant friction of cylindrical designs. This pulsating stirring is extremely effective in fracturing the oxide layers and generating vertical flow in the rapidly cooling plasticized zone. The welded joint made with the straight hexagonal profile tool ultimately produced the highest tensile strength, 302 MPa, and the best joint efficiency. This confirms that maximizing the swept dynamic volume is crucial under UFSW conditions.

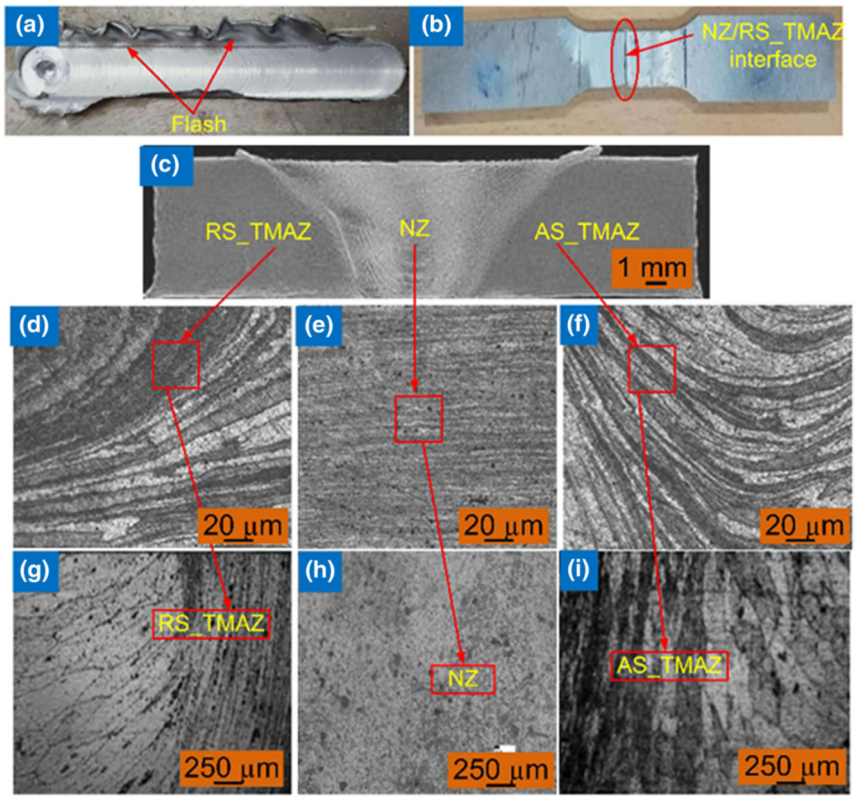

Figure 17. (a) UWFSW fabricated by SH (b) ASTM-E8 tensile tested specimen (c) macrostructures of welds (d) microstructure at RS-TMAZ (e) NZ (f) AS-TMAZ, (g) high magnification (500X) at RS-TMAZ (h) NZ and (i) AS-TMAZ [102].

Although UFSW improves the properties of welded joints, post-weld heat treatments can further enhance joint performance. Dong et al. [103] evaluated the effects of post-weld heat treatment on different underwater joints of 7003-T4 and 6060-T4 aluminum and concluded that a subsequent aging treatment would be necessary to reprecipitate the strengthening phases that partially dissolved during welding, even though the underwater process successfully minimized the width of the softened zone. Using transmission electron microscopy, it was confirmed that a solution treatment plus artificial aging (STA) regimen successfully repopulated the matrix with fine η and β precipitates, eliminated the characteristic hardness minimum in the HAZ, and restored the material in the joint to levels close to those of the base material. Combining UFSW with targeted heat treatments provides a reliable route to producing high-performance joints in complex, heat-treatable alloys.

3.2. Ultrasonically Assisted Friction Stir Welding (UaFSW)

Ultrasound-assisted friction stir welding (UaFSW) emerged to reduce the high reaction forces that occur during the process, which lead to severe tool wear that accompanies conventional FSW, in

 doi:10.20944/preprints202605.1246.v1

the case of hard alloy joints. By superimposing high-frequency vibrations of the FSW process, typically around 20 kHz, on either the tool or the workpiece, the technique fundamentally modifies the material rheology and frictional behavior.

Fan et al. [104] identified the "acoustoplastic effect" which, by introducing ultrasonic energy during the welding process, reduces the static yield stress of the metal, allowing plastic deformation at substantially reduced applied loads. The mechanism operates at the level of the crystal lattice, with dislocations absorbing acoustic energy, facilitating their movement and multiplication, effectively softening the material without additional heat input. Both plunge and traverse welding forces are significantly lower than in standard FSW, which helps to extend tool life and makes it possible to machine much harder alloys.

Muhammad et al. [105] observed that in Al/Mg dissimilar joints welded with ultrasonic assistance, a more homogeneous mixing of the materials and a flattening of the thermal gradient in the weld zone are achieved, which causes the residual stress to decrease. Both numerical models and experimental measurements confirmed that ultrasonic vibrations reduced the peak longitudinal residual stress on the aluminum side by approximately 25% compared to conventional friction stir welding (FSW) - a reduction mainly driven by enhanced dynamic recrystallization, which actively alleviates internal lattice deformations.

Zhao et al. [106] analyzed the microstructural changes at the Al/Mg bonding interface and found that the ultrasonic field actively fragments continuous IMC layers. High-frequency vibrations cause cavitation and acoustic flow in the plasticized metal, breaking the fragile phases into discrete particles and eliminating continuous crack propagation paths that undermine the joint's ductility. As schematically illustrated in Figure 18, acoustic energy propagates through the sonotrode, generating transient cavitation bubbles in the semi-solid material. When these bubbles collapse, the resulting localized shock waves mechanically fracture the continuous layers of $Al_{12}Mg_{17}$ and Al_3Mg_2, while the acoustic flow removes the fragments from the interface.

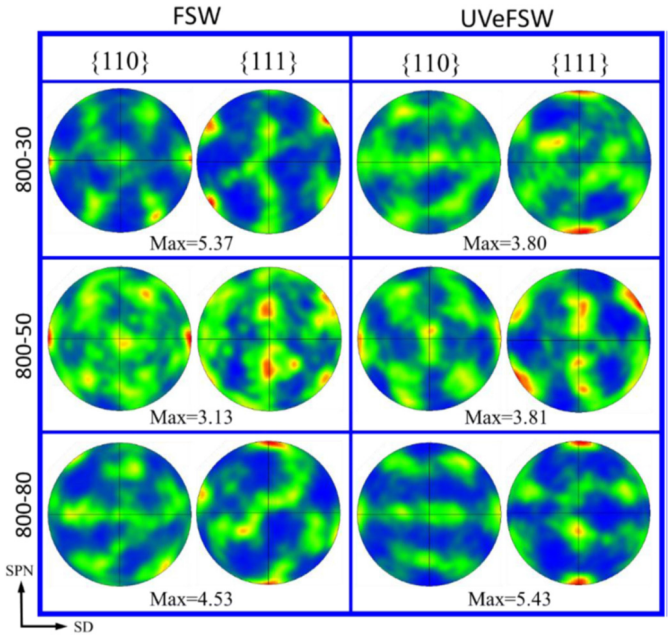

Figure 18. {101} and {111} pole figures at location A3 (the WNZ in the Al side) under different weld speeds. SPN-shear plane normal, SD-shear direction [106].

Tunnel voids, also called wormholes, are among the most common defects that occur in FSW, typically forming when the material flow on the advancing side is insufficient to fill the cavity left behind the pin. Wu et al. [107] applied a coupled thermomechanical model to investigate this problem in UaFSW, showing that ultrasonic vibration locally increases both the strain rate and the material velocity around the tool pin. The improved fluidity ensures that the back cavity is completely filled,

 doi:10.20944/preprints202605.1246.v1

suppressing void formation even at high welding speeds, confirming that the superimposed ultrasonic vibration widens the plasticized flow path, and the material flow velocity at the tool-workpiece interface increases directly proportional to the ultrasonic amplitude.

Qian et al. [108] investigated the impact of ultrasonic treatment (UIT) on 2219 aluminum alloy joints, observing that ultrasonic energy refines the grain structure of the agitated zone and redistributes hardening precipitates. This microstructural refinement reduces the electrochemical potential difference between grain boundaries and the grain interior, reducing susceptibility to intergranular corrosion. The treatment also induces a deep layer of compressive residual stress which, combined with the dissolution of continuous precipitates at the grain boundaries, effectively seals potential corrosion channels.

Ambrosio et al. [109] explored the use of acoustic emission (AE) monitoring in FSW, demonstrating that in hybrid processes, the technique can characterize the real-time interaction between the tool and the workpiece, rather than simply detecting defects. Analysis of the acoustic signature, particularly the burst signals associated with friction and material detachment, provides immediate feedback on the stability of the acousto-plastic flow, allowing adaptive control of welding parameters and allowing operators to correct adverse conditions before they compromise the joint.

3.3. Other Variants: Stationary Shoulder and Energy-Assisted FSW

In addition to ultrasonic and underwater welding methods, the field of FSW now includes tool-specific and energy-assisted variants, tailored to address specific metallurgical constraints. Saha et al. [110] analyzed these externally energy-assisted methods, classifying them according to the source of additional heat: laser, induction, or electric arc. Their main argument is that, for high-melting-point materials, preheating the workpiece is essential to reduce the flow stress at the tool face, minimizing tool wear and preventing pin failure. These hybrid techniques effectively disconnect heat generation from the material flow, allowing independent control over the thermal cycle and the rate of plastic deformation.

3.3.1. Stationary Shoulder Friction Stir Welding (SSFSW)

In the conventional FSW process, the rotating shoulder serves both as a heat source and as a forging element. These roles can be optimized independently through the stationary shoulder FSW (SSFSW) process. This process solves this problem by allowing the shoulder to slide over the workpiece while the internal pin rotates independently, transforming the shoulder from a heat source into a heat sink. Sundar et al. [111] used a static shoulder tool to join AA6061 aluminum, demonstrating that the reduced heat input produces a narrower heat-affected zone (HAZ) and a finer crystallographic texture. EBSD analysis showed that the static shoulder creates a unique deformation path, dominated by simple shear texture components (B/B̄), significantly reducing the coarse-grained structure.

Sun et al. [112] applied SSFSW to 2A97 aluminum-lithium alloys, achieving a mirror-like, nearly burr-free surface finish. Microstructural characterization showed that the stationary shoulder prevents the coarsening of hardening precipitates near the surface, resulting in a more uniform distribution of hardness across the plate thickness. The surface layer develops a specific shear microstructure due to the sliding shoulder, while the center is dominated by pin-shear, creating a complex sandwich-type microstructure that improves damage tolerance and fatigue resistance. As schematically illustrated in Figure 19, the non-rotating shoulder slides smoothly over the joint line, applying forging pressure to keep the material plasticized, while the independently rotating pin generates heat through localized friction and mixing, creating a clear separation between mechanical forging and thermal agitation, which constitutes the fundamental principle behind the process's precision characteristics.

 doi:10.20944/preprints202605.1246.v1

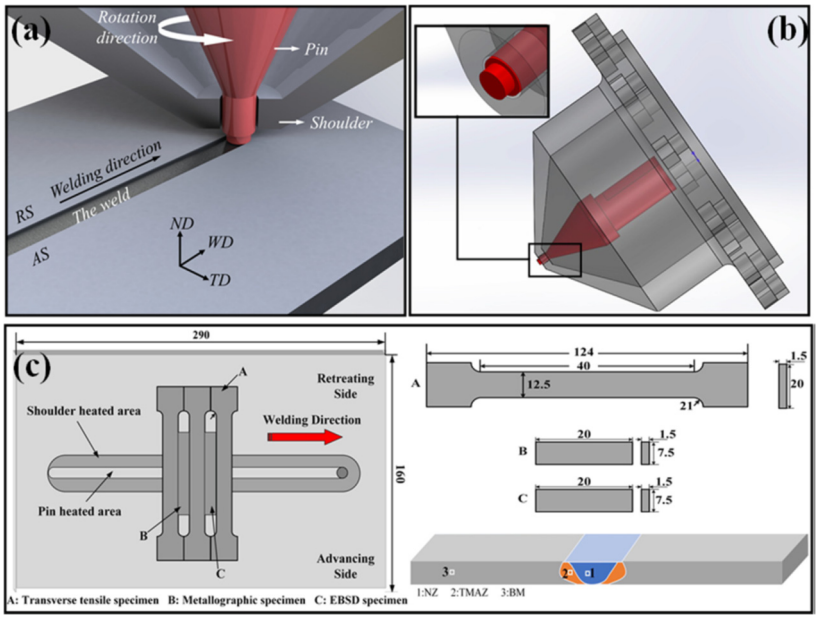

Figure 19. Schematic illustration of the (a) SSFSW process; (b) welding tool employed in the trials; (c) locations and dimension of transverse specimen [112].

3.3.2. Laser and Induction-Assisted Hybrid Processes

For materials with high melting points, optical and electromagnetic energy sources are increasingly being integrated into the FSW process. Gong et al. [113] investigated a hybrid method that combines FSW with Laser Shock Peening (LSP) on dissimilar joints made of titanium and aluminum alloys. Although the laser does not directly participate in the welding, post-weld laser peening introduces compressive residual stresses that effectively counteract stress corrosion cracking, the primary failure mode in dissimilar titanium-aluminum welds. High-energy laser pulses generate plasma shock waves that cause severe plastic deformation at the surface, neutralizing the harmful tensile stresses produced during the welding heat cycle, while simultaneously refining the surface grains into a nanostructured layer. This layer blocks the diffusion pathways required for the permeation of corrosive hydrogen, thereby inhibiting crack initiation.

Induction-assisted FSW is another important method for joining superalloys and steels. Raj et al. [114] evaluated the impact of induction preheating on dissimilar joints between Inconel 718 and SS316L, finding that the local increase in the base material's temperature prior to stirring allowed for the material to flow properly, without the catastrophic tool degradation typically associated with cold joining of hard alloys. Electrochemical analysis showed that this thermal management strategy suppresses the precipitation of the harmful Laves phase in the nugget zone, providing corrosion resistance comparable to that of the base metal and a significant improvement over conventional processing. In a follow-up study, Raj et al. [115] analyzed the mechanical properties of these joints, noting that preheating encourages dynamic recrystallization, refining the grain structure and improving interfacial ductility. As illustrated in Figure 20, the induction coil is positioned immediately in front of the rotating tool, ensuring that the Inconel and steel substrates are softened to a ductile state just before the tool engages, thereby reducing the yield stress and protecting the tool from severe abrasive wear.

 doi:10.20944/preprints202605.1246.v1

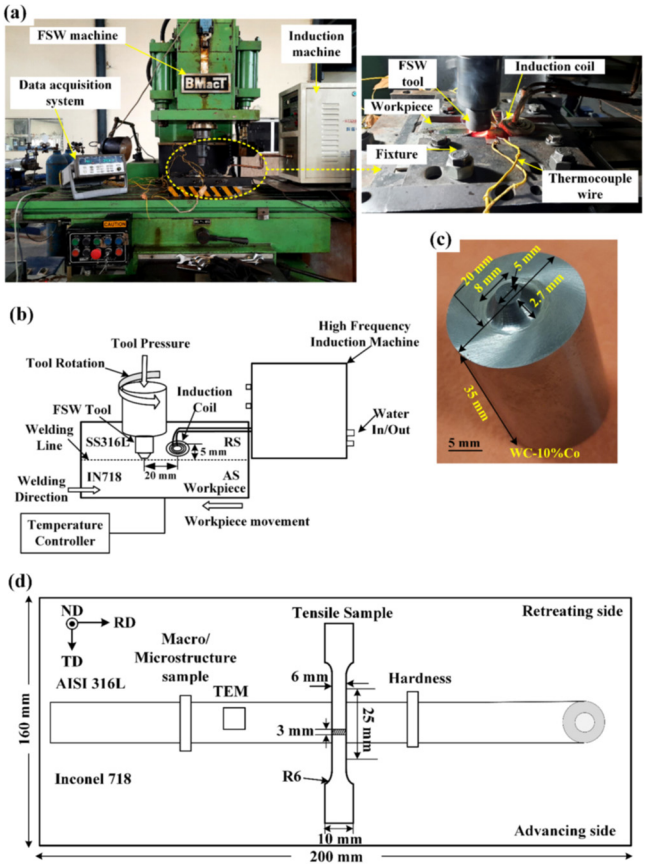

Figure 20. (a) Experimental setup of induction-assisted FSW (I-FSW) system, (b) schematic diagram of I-FSW, (c) Wc-10%Co FSW tool and (d) Schematic diagram of extraction of testing specimens [115].

4. Digitalization and Industry 4.0 in FSW

Variations of the friction stir mixing process are also used in advanced surface engineering. Aliabadi et al. [116] demonstrated this by combining flame spraying with the friction stir mixing (FSP) process. After depositing a wear-resistant NiCrBSi layer, FSP was applied to consolidate the material, eliminating the porosity and lamellar defects that typically affect thermal spray-applied layers. The resulting coating was completely dense and metallurgically bonded to the substrate, which is clear evidence that friction-based mechanisms offer substantial industrial value, far exceeding that of conventional joining.

The integration of Industry 4.0 principles into the solid-state joining process represents a decisive shift from empirical, trial-and-error methodologies toward predictive digital frameworks. Within this paradigm, numerical modeling and simulation have become essential tools for deciphering the complex thermomechanical physics of the FSW process.

4.1. Numerical Modeling and Simulation (FEM/CFD)

The primary objective of numerical simulation in FSW is to predict temperature gradients, material flow trajectories, and potential defect formations without the associated costs of physical prototyping. Akbari et al. [117] observed that, while traditional Lagrangian methods work adequately for basic thermal analysis, arbitrary Lagrangian-Eulerian (ALE) and coupled Eulerian-Lagrangian (CEL) formulations are much better equipped to handle the extreme mesh distortion caused by severe plastic deformation.

4.1.1. Heat Generation and Thermomechanical Behavior

Accurate prediction of heat generation is the foundation of any FSW simulation. Using a CEL-based finite element method, Salih et al. [118] analyzed heat generation and plastic flow in aluminum

 doi:10.20944/preprints202605.1246.v1

alloys, finding that maximum temperatures are localized directly under the shoulder of the tool. Their models also revealed that the residual stress profile is highly asymmetric and depends largely on clamping constraints and cooling rates. The maximum longitudinal residual stress peaks at the weld centerline and is approximately 40–50% of the material's yield strength.

Capturing the exact mechanisms of defect formation requires more sophisticated multiphysical approaches. Shi et al. [119] introduced a thermal-fluid-structural coupling model to study the generation of voids, treating the plasticized metal as a non-Newtonian fluid while simultaneously calculating the structural response of the tool. Their approach accurately predicted the occurrence of tunnel-type defects, directly correlating them with the inadequate vertical flow of material on the feed side. As illustrated in Figure 21, the simulation clearly reproduces the morphology and position of a "wormhole" defect; thus, at high feed rates, the material flow is simply too slow to fill the cavity behind the pin, producing a volumetric void that aligns precisely with the metallographic results.

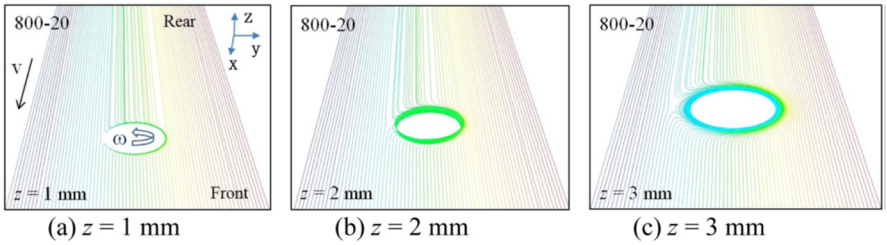

Figure 21. The macroscopic plastic material flow at the rotational speed of 800 rpm and welding speed of 20 mm/min [119].

By implementing a spatially variable friction model, in which the friction coefficient dynamically adapts to local temperatures and slip rates, Yang et al. [120] demonstrated that static friction predominates in the hot center of the shoulder, while sliding friction occurs at the cooler outer edges. This is a distinction that standard Coulomb friction models systematically ignore, and its omission introduces significant errors in torque predictions.

Ji et al. [121] observed that specific geometric features of the tool contribute differently to the overall heat generation. They isolated the effects of the shoulder and the pin in their numerical models, finding that while the shoulder accounts for up to 80% of the total heat input, the characteristics of the pin—threads, flat surfaces, and similar surface features—determine the vertical mixing necessary to prevent root defects. Based on this, Akbari et al. [122] quantified the deformation generated by the individual components of the tool, finding that the strain rate reaches maximum values at the tip of the pin, a detail with direct implications for the design of tools intended for difficult-to-weld alloys.

The accuracy of FSW simulations also depends on the choice of friction law. Liu and Sun [123] argued that internal viscous dissipation plays a major role in heat generation, proposing a vortex-FSW simulation based on internal friction rather than solely on surface interactions. To further refine the boundary conditions, Liu et al. [124] developed an FEM model in which they accounted for the temperature-dependent friction coefficient. By dynamically adjusting friction in response to localized thermal changes, their method achieved significantly closer correspondence between simulated and experimental thermal cycles than models with constant friction.

4.1.2. Material Flow and Defect Prediction Using CEL

The coupled Eulerian-Lagrangian method has become the preferred approach for modeling extreme deformations in FSW, as highlighted by Laska et al. [125], who applied CEL to evaluate how tool geometry influences temperature and material flow in AA6082 aluminum, successfully visualizing the formation of "onion rings" and confirming that the periodicity of material deposition is directly controlled by the tool shape. Akbari et al. [126] mapped the strain and temperature distributions during FSW of AA5083 and AA7075, their CEL model correctly predicting that although higher rotational speeds expand the volume of the agitation zone, they also trigger excessive temperature if the plunge depth is not carefully calibrated. Defect prevention is ultimately the main

 doi:10.20944/preprints202605.1246.v1

goal of these simulations. Choudhary and Jain [127] used CEL to track undercut tunnel defects, confirming that they arise from a fundamental imbalance between the material pushed outward by the pin and the holding pressure exerted by the shoulder. Turkan and Karakas [128] reinforced this conclusion by showing that numerical models can identify the exact combinations of feed and rotation speeds that produce voids, defining a safe process zone in a virtual environment.

4.2. Machine Learning and Artificial Intelligence

Machine learning and artificial intelligence handle nonlinear process complexity in ways that traditional analytical models simply cannot match.

4.2.1. Overview and Real-Time Defect Detection

In a critical review of machine learning applications in FSW, Elsheikh [129] organized current efforts into three main areas: joint property prediction, real-time process control, and tool failure diagnosis. The review makes an important observation: while conventional finite element models are computationally expensive, trained machine learning algorithms can provide near-instantaneous predictions. One of the most significant practical demonstrations of this capability comes from Guan et al. [130], who developed a machine learning framework driven by force data to identify internal flaws such as tunnels and voids. By training their algorithms on dynamic fluctuations in axial and transverse forces, they achieved high classification accuracy, showing that force signals carry a characteristic fingerprint corresponding to specific defect states.

4.2.2. Predictive Modeling of Mechanical Properties

The largest body of ML work in the FSW field focuses on predicting ultimate tensile strength and related mechanical properties. Anandan and Manikandan [131] applied various regression models to predict ultimate tensile strength (UTS) in AA2050-T8 joints, using K-Fold cross-validation to ensure robustness. Their approach demonstrated that data-driven methods can reliably relate rotation and traverse speeds to ultimate joint strength, effectively acting as a virtual testing laboratory. In a subsequent study, Anandan and Manikandan [132] adapted this methodology to predict peak temperatures in joints between AA7050 and AA2014A. Their methodology is valuable from a practical point of view because temperature directly governs the dissolution of hardening precipitates, and their model eliminated the need for embedded thermocouples. Verma et al. [133] extended machine learning modeling to aircraft-grade alloys, mapping the complex relationships between tool rake angle and the resulting microhardness profile in high-strength aluminum systems.

4.2.3. Comparison of Algorithms and Advanced Architectures

Research has progressively moved beyond simple regression and toward more systematic comparisons of algorithm architectures. Mysliwiec et al. [134] evaluated Random Forest, XGBoost, and Multilayer Perceptron neural networks for optimizing welding of AA2024-T3 aluminum, finding that ensemble methods such as XGBoost frequently outperform individual neural networks when processing noisy experimental data typical of real welding trials. Neural networks are particularly effective when optimizing for multiple simultaneous objectives. Nejad et al. [135] designed an artificial neural network to evaluate fatigue life in AA2024-T351 joints, combining it with multi-objective optimization algorithms to identify process parameters that maximize fatigue life while minimizing residual stresses.

4.2.4. Deep Learning and Ensemble Methods

Rabe et al. [136] applied deep learning to force feedback signals to detect void defects. Unlike conventional machine learning approaches, which require manual feature extraction, their model automatically learned the hierarchical features embedded in the force signal, which is a more robust solution for quality assurance. To improve the prediction accuracy in asymmetric welding

 doi:10.20944/preprints202605.1246.v1

configurations, Matitopanum et al. [137] used ensemble methods, superimposing multiple weak predictive models into a single strong learning model and substantially improving UTS predictions for complex joint geometries. The result emphasizes the principle that managing the inherent stochasticity of FSW requires algorithmic architectures that are sophisticated enough to capture it.

4.3. Statistical Optimization Techniques

Statistical optimization methods remain fundamental to experimental design in FSW. They provide the framework that links input parameters, such as rotation speed, traverse speed, tool tilt, to measurable outputs, such as tensile strength, microhardness, and grain size, allowing researchers to determine optimal process parameters without exhaustive physical testing.

4.3.1. Overview of Optimization Strategies

Prabhakar et al. [138] reviewed measurement and optimization strategies in FSW, arguing that the stochastic nature of material flow requires robust statistical frameworks to contain experimental variance. The traditional trial-and-error approach is too inefficient for industrial-scale reliability, making structured design of experiments essential. Asadi et al. [139] reinforced this with a multivariate study that simultaneously optimized mechanical and microstructural properties, demonstrating that targeting a single objective, such as tensile strength, for example, often comes at the expense of corrosion resistance or ductility, making multi-objective formulations a practical necessity.

4.3.2. Response Surface Methodology

Akbari and Asiabaraki [140] combined RSM with the Nondominated Sorting Genetic Algorithm (NSGA-II) to optimize tool parameters for aluminum lap joints, navigating the objectives of maximizing joint strength while minimizing sheet thinning and burr formation. For dissimilar joints, where process interactions are more complex, RSM proved equally valuable. Jain et al. [141] developed a second-order regression model for AA6061/AA7075 composite joints that accurately captured the interaction between rotation speed and tool rake angle. Haribalaji et al. [142] applied RSM to dissimilar AA2014 and AA7075 joints, identifying rotation speed as the dominant factor governing metal mixing. Extending this to microstructural management, Ramamurthy et al. [143] used RSM to directly link process parameters to grain size and microhardness in AA2014/AA6063 welds, while Akbari et al. [144] applied the methodology to optimize friction stir machining of piston alloys for maximum wear resistance.

4.3.3. Taguchi Method and Grey Relational Analysis (GRA)

The Taguchi approach remains highly regarded for its effectiveness in reducing experimental volume through signal-to-noise analysis. Boukraa et al. [145] extended this method by coupling Taguchi models with Grey relational analysis, translating competing performance indicators, such as elongation and tensile strength, into a unified Grey relational degree that simplifies the optimization of complex joint characteristics. Researchers have increasingly coupled these statistical foundations with meta-heuristic algorithms. Kahhal et al. [146] combined RSM with Particle Swarm Optimization (PSO) to identify parameter combinations that maximize the strain rate while keeping peak temperatures low, with PSO converging to the global optimum noticeably faster than conventional gradient descent. Karumuri et al. [147] confirmed the value of Taguchi-based GRA for different aluminum welds, demonstrating its ability to handle highly nonlinear relationships between tool geometry and traverse speed.

4.3.4. Validation of High Strength and Marine Alloys

Kumar et al. [148] applied RSM to maximize the strength of FSW welded joints for AA6082 and AA7050, while Mehdi et al. [149] adopted a multiple response RSM strategy for welding different

 doi:10.20944/preprints202605.1246.v1

AA2014/AA6061 materials. A consistent conclusion of both studies is that the optimal processing parameters are strictly material dependent. Thus, the 7xxx series alloys require distinctly lower heat inputs than their 6xxx counterparts to avoid dissolution of critical strengthening precipitates. The design of the statistical matrix itself also matters. Abd Elnabi et al. [150] tested various Taguchi orthogonal matrices during welding of different Al alloys, finding that the chosen matrix strongly influences the statistical reliability of the result. Ahmed et al. [151] took this work towards direct industrial applications, adapting FSW parameters for marine-grade AA5451 and establishing a precise operational envelope that satisfies stringent marine certification requirements.

5. Microstructural Challenges and Defect Characterization

The mechanical reliability of an FSW joint ultimately depends on the microstructural changes induced by severe thermomechanical cycling. Since FSW operates entirely in the solid state, the integrity of the joint is not governed by solidification mechanics, but by Dynamic Recrystallization and the dissolution and reprecipitation of the strengthening phases, processes that are sensitive to small variations in thermal history and much less permissive than it might initially appear.

5.1. Microstructural Evolution

5.1.1. Dynamic Recrystallization and Grain Growth

Intense plastic deformation in the stir zone typically produces a refined, equiaxial granular structure through continuous dynamic recrystallization. This refined state is, however, thermodynamically unstable. Kalinenko et al. [152] found in AA6061-T6 that abnormal grain growth frequently occurs during post-weld cooling or subsequent heat treatments. As the precipitates that normally fix the grain boundaries dissolve, these boundaries migrate rapidly, leaving behind a heterogeneous microstructure that can severely compromise ductility.

Figure 22 from Baghdadi et al. [153] illustrates the extent of this transformation in post-weld heat-treated joints, along the advancing side, the agitation zone, and the retreating side. The micrographs show a significant change after heat treatment, with the initially fine grains in the agitation zone undergoing massive abnormal expansion, swelling to hundreds of micrometers or even millimeters and effectively swallowing the adjacent thermomechanical affected areas. The result is an illustration of the fragile thermodynamic equilibrium between the driving forces of migration at grain boundaries and the retarding effect of second-phase particle dissolution.

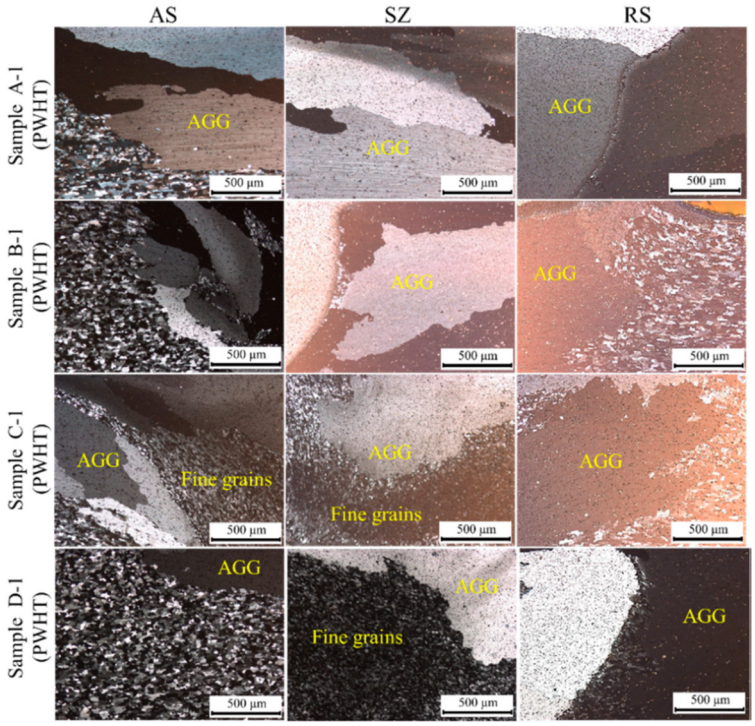

 doi:10.20944/preprints202605.1246.v1

Figure 22. AGG occurs in the microstructure of PWHTed Al5083-l6061 (T6) at a constant travel speed of 100 mm/min [153].

Rajendran et al. [154] addressed the fatigue implications of this microstructural discontinuity in AA2024-T6, finding that an optimized post-weld heat treatment can homogenize the precipitate distribution and delay crack initiation even when coarse grains are present.

5.1.2. Precipitation Behavior and Corrosion Susceptibility

The thermal cycling imposed during FSW fundamentally alters the precipitation state of heat-treatable aluminum alloys, causing dissolution in the stir zone and coarsening of precipitate grains in the stir zone. Non-heat-treatable alloys face a different problem, called thermal sensitization. Ning et al. [155] characterized the precipitation of the anodic β phase (Al_3Mg_2) along grain boundaries in AA5083, noting that FSW parameters directly control the phase continuity. A network connected at grain boundaries leaves the alloy extremely vulnerable to intergranular corrosion.

In the case of high-strength 7xxx alloys, Guo et al. [156] showed that retrogression and re-aging treatments can disrupt the connectivity of grain-bound precipitates in Al-Zn-Mg-Cu joints, improving the stress corrosion cracking resistance without compromising the tensile strength. In dissimilar joints, galvanic coupling becomes the dominant corrosion mechanism, thus, Lu et al. [157] studied the corrosion behavior in dissimilar aluminum joints, finding that the sharp microstructural gradient at the interface establishes a localized galvanic cell that promotes preferential corrosion in the affected surface area of the more anodic material.

Figure 23 from Wang et al. [158] illustrates how FSW welding addresses these vulnerabilities through three simultaneous modifications: physical flattening of the surface to reduce exposure to corrosive media, replacement of the tensile residual stresses with a compressive layer, going from +58.3 MPa to -25.7 MPa at the weld periphery, and forcing a discontinuous distribution of fine precipitates across the grain size while narrowing the precipitate-free zones. Together, these modifications interrupt the active micro-galvanic pathways responsible for localized attack.

In a similar approach, Meng et al. [159] demonstrated that multi-pass friction stir remanufacturing can refine coarse precipitates and eliminate pre-existing micro-defects, restoring the fatigue strength of the material.

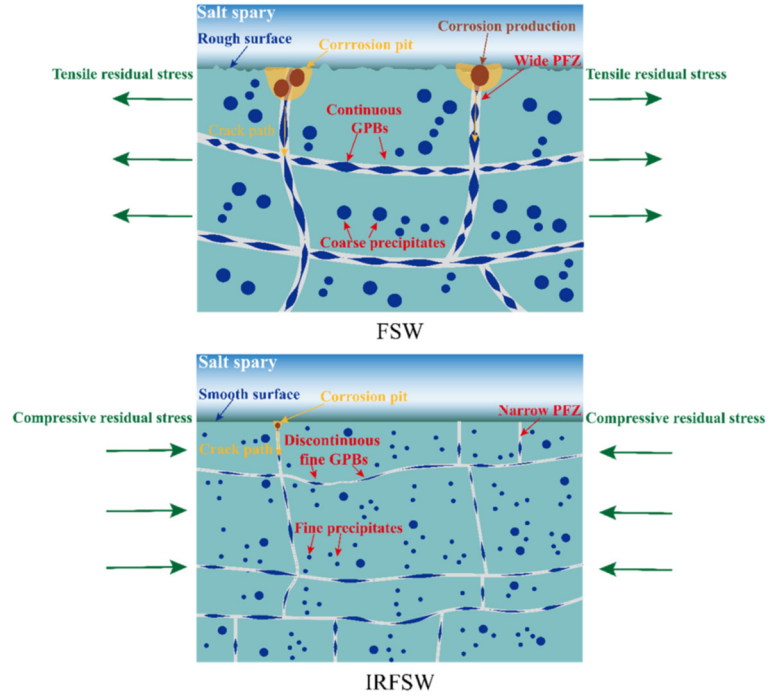

Figure 23. Schematic of corrosion resistance mechanism of IRFSW joint [158].

 doi:10.20944/preprints202605.1246.v1

5.1.3. Influence of Welding Speed and Texture

The traverse speed largely controls the heat input during friction stir welding and, thereby, the degree of precipitate dissolution. Kim et al. [160] found a direct relationship between welding speed and the strengthening mechanisms in the case of 7075 aluminum alloy. High traverse speeds reduce the net heat input and restrict the coarse growth of η precipitates in the heat affected zone (HAZ), which is the area with the lowest mechanical strength of the joint. Mohammadi-pour et al. [161] have highlighted this in aerospace-grade 7075-T6 welds, emphasizing that a narrow thermal cycle is essential to maintain high joint efficiency.

Figure 24 from Kesharwani et al. [162] captures the crystallographic consequences of severe thermomechanical deformation in AA7075-T6, observing strong concentrations of the A_1^*/A_2^* and $A/\bar{A}$ shear texture components in the polar figures and orientation distribution functions. These intense localized textures, driven by dynamic recrystallization and rotating tool kinematics, create planes of crystallographic weakness that ultimately dictate the macroscopic fracture path under tensile loading.

Mehri et al. [163] translated these structural changes into sheet forming behavior, showing that the altered structure of the stir zone generally decreases local formability relative to the unaffected base metal.

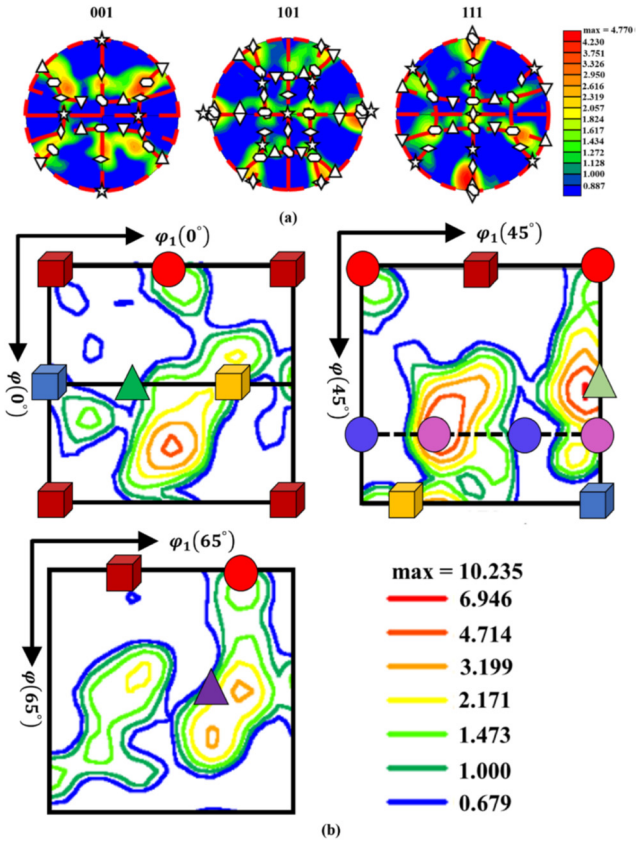

Figure 24. Superimposed ideal shear texture component on AA7075-T6 plate weld using square-shaped pin: (a) PF, and (b) Orientation distribution function sections at φ2 = 0◦, 45◦, and 65◦, respectively. [162].

5.1.4. Advanced Alloys and Thermal Cycling

In the case of ultrathin sheets, Ni et al. [164] showed that high-speed friction stir welding (FSW) on AA7075-T6 sheet produces very short thermal cycles that prevent complete dissolution of the precipitate, resulting in a specialized microstructure that retains much of the original hardness of the base alloy. Tang et al. [165] noted that process kinematics also shape microstructural symmetry and found that alternating tool rotation direction during friction stir welding (FSW) on both sides of 6061

 doi:10.20944/preprints202605.1246.v1

aluminum produces an interlaced grain architecture that eliminates the weak interface line characteristic of standard lapped welds. Liang et al. [166], noting that post-weld treatments continue to extend the operational limits of FSW, subjected 6N01 alloy joints to electro-pulsing combined with artificial aging, finding that the applied electrical pulses accelerated the nucleation of nanoprecipitates and led to a rapid recovery of tensile strength. For lithium-alloyed systems, the thermal sensitivity of the T1 hardening phase requires strict cooling protocols. Tao et al. [167] showed that immediate water quenching followed by artificial aging is mandatory for 2198-T8 Al-Li joints to preserve this phase, a finding confirmed by the more extensive analysis of Al-Li thermal degradation by Yang et al. [168].

At the tool level, Figure 25 in Hou et al. [169] illustrates a geometry that incorporates the eccentricity of the pin. By offsetting the central axis of the pin with respect to the axis of rotation of the shoulder, the tool generates a pulsating stirring motion with an extended volume. This forces chaotic and asymmetric mixing of the plasticized metal, fragments persistent oxide layers, and leads to superior metallurgical consolidation compared to conventional concentric designs.

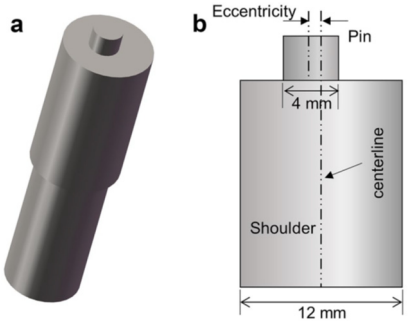

Figure 25. Schematic illustration of the tool geometry (a), pin eccentricity and tool dimensions (b) [169].

5.2. Intermetallic Compound Formation

In joining dissimilar materials, the precipitation and growth of intermetallic compounds represent the main metallurgical bottleneck, and their kinetics are governed almost entirely by the peak temperatures and diffusion times, both of which are set by the chosen welding strategy. Jain et al. [170] examined multi-pass welding in different AA6082 and AA5083 joints, finding that while successive passes improve the macroscopic homogeneity, repeated thermal cycling accelerates the diffusion of alloying elements and SiC microparticles at the interface. Without careful thermal management, this prolonged exposure significantly thickens the brittle reaction layer.

Hashmi et al. [171] highlighted that structural defects in welded joints originate from inadequate heat input or disturbed material flow and, in a wear analysis of AA6082/SiC composites, showed that progressive tool wear changes the pin profile during operation, compromising the stirring action and ultimately generating subcutaneous voids. Salah et al. [172] applied EBSD to multi-pass friction stir processing of Si-rich TIG welded dissimilar joints, confirming that the flow pattern, fundamentally governed by whether the harder or softer alloy occupies the advancing side, controls both the degree of mechanical mixing and the local stoichiometry of the resulting IMCs. Mabuwa et al. [173] confirmed this in AA6082/AA8011 configurations, showing that strategic material positioning alters the heat input distribution and suppresses continuous and brittle intermetallic networks. Habba et al. [174] demonstrated that when joining AA5083-H111 by the FSW process, it provides superior joint integrity and measurable economic advantages over the MIG and TIG alternatives. The fundamental mechanics of the process, however, remain very sensitive to parameter selection. Basak et al. [175] found that pre-existing interfacial oxide layers in rolled aluminum sheets can be entrained in the agitation zone, agglomerating into zigzag defects that readily initiate fractures. Uday and Rajamurugan [176] have summarized the broader implications of flow-related defects, emphasizing that a viable process window depends entirely on the balance between the rotational speed, which

 doi:10.20944/preprints202605.1246.v1

governs heat generation, and the traverse speed, which governs the cooling rate. Operation outside this envelope produces either cold weld defects, such as tunnel voids, or hot weld defects, such as excessive burr. Tool kinematics add an additional degree of control, as emphasized by Meyghani and Awang [177], who identified the tool tilt angle as a key variable governing thermomechanical behavior and heat generation in the stir zone. To address complex geometries and dimensional inaccuracies, Dong et al. [178] introduced wire-based FSW, which actively feeds and shears the filler material downward to bridge the assembly gaps and maintain joint strength despite structural discontinuities. The performance of the joints can be further improved by specific compositional adjustments and post-weld surface treatments. Qiu et al. [179] showed that Al-Mg microalloying systems with scandium and zirconium produce fine and coherent $Al_3(Sc,Zr)$ dispersoids, which counteract the loss of yield strength and increased susceptibility to corrosion normally induced by FSW thermal cycling. From a surface engineering perspective, Chen et al. [180] applied Ni-P duplex coatings over an anodic aluminum oxide interlayer, significantly improving the wear and corrosion resistance of 6061-T6 FSW joints in aggressive environments.

Systems characterized by extreme metallurgical incompatibility, such as steel-magnesium joints, require specialized tooling strategies, as noted by Khalaf et al. [181], who investigated the effect of the number of tool shoulders, ranging from one to four, finding that frictional heat generation increases with the number of shoulders up to a critical threshold. A two-shoulder configuration was found to be optimal, providing sufficient thermal energy for solid-state bonding without causing massive elemental degradation or leading to excessive growth of Fe-Mg intermetallic.

Figure 26 of Kumar et al. [182] illustrates a friction stir butt welding configuration using a zinc foil interlayer pre-placed between aluminum and magnesium plates. As the rotating tool advances along the joint line, it thermomechanical plasticizes the zinc barrier and sweeps it into the stir zone, preventing direct atomic contact between the two base metals and replacing the brittle Al-Mg intermetallic compounds with more mechanically favorable Zn-rich binary and ternary compounds, a substitution that directly translates into higher overall joint strength.

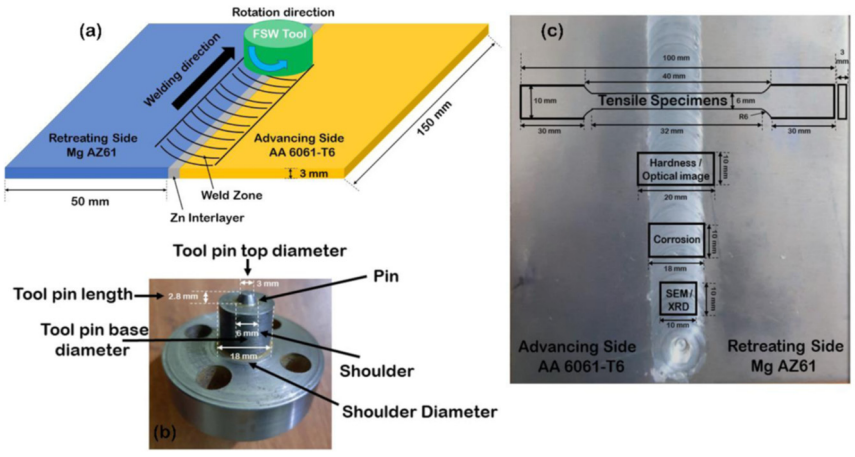

Figure 26. (a) A schematic representation of the friction stir butt welding (FSBW) methodology with Zn interlayer, (b) FSW tool, (c) Dimensional illustration of test specimens [182].

Qian et al. [183] applied ultrasonic impact treatment to AA2219 joints and found that the resulting surface nano-crystallization, combined with a compressive residual stress layer, substantially improved the resistance to stress corrosion cracking, a result that points to surface engineering as a viable complement to parameter optimization when corrosion performance is a priority. The inherently solid nature of friction-based techniques gives them a great advantage in additive manufacturing, especially in terms of component density. Shen et al. [184] demonstrated that friction-based additive manufacturing produces fully dense Al-Li structures, avoiding the gas porosity that persistently compromises fusion-based alternatives such as wire-arc additive

 doi:10.20944/preprints202605.1246.v1

manufacturing, a problem that Yi et al. [185] noted requires complex mitigation strategies that add cost and complexity to the process. Friction-assisted additive manufacturing represents a truly competitive path to producing defect-free, corrosion-resistant structural parts, rather than a mere academic curiosity. Hybrid processing strategies add an additional degree of control over thermal cycling and phase evolution, as highlighted by Zhao et al. [186], who found that ultrasonic vibration-enhanced FSW (UVeFSW) profoundly influences both intermetallic compound development and dynamic recrystallization in Al/Mg joints. Acoustic energy physically breaks down continuous, brittle IMC layers into isolated particles, stopping macroscopic crack propagation pathways that would otherwise form, while simultaneously refining the grain structure of the weld nugget and improving the overall ductility of the joint. The two effects are complementary, with fragmented IMCs eliminating the primary fracture pathway, and granular refinement increasing the energy required to propagate any crack that does initiate.

6. Conclusions and Future Perspectives

6.1. Summary of Main Findings

During this review, several developments stand out as truly important for the field:

- Joining dissimilar materials.

The ability to reliably join metallurgically incompatible systems, aluminum with steel, magnesium or copper. is probably the most significant industrial achievement of friction stir welding (FSW). The viability of these joints depends almost entirely on maintaining the intermetallic compound layers below critical thickness thresholds, generally below 10 μm, to preserve ductility. Achieving this in practice requires strict adherence to optimized process parameters or deliberate tool offset positioning.

- Process variants.

Underwater FSW and ultrasonically assisted FSW have each addressed specific limitations of the conventional process.

UFSW offers aggressive thermal management for heat-sensitive alloys, effectively limiting strength loss in the heat-affected zone. UaFSW reduces processing forces and improves material flow, making it more practical to weld complex geometries while extending tool life, a combination that has significant implications for manufacturing economics.

- From joining to manufacturing.

Perhaps the most telling sign of FSW's maturity is that its basic principles now extend far beyond joining. Friction Stir Processing has established itself as a robust tool for surface engineering and composite synthesis. Friction Stir Additive Manufacturing, meanwhile, offers a solid-state alternative to fusion-based additive manufacturing, capable of depositing fully dense materials equivalent to forging, without the defects of porosity and solidification.

6.2. Future Outlook

Despite these constraints, the direction of travel for solid-state joining is reasonably clear, and it points toward hybrid, additive, and digitally integrated manufacturing.

The incorporation of auxiliary heat sources, lasers, induction coils, and electrical arcs, is expected to become standard practice for high-strength alloys. By preheating the workpiece, these hybrid systems lower the material's flow stress ahead of the tool, simultaneously protecting the tool from excessive wear and boosting traverse speeds without compromising joint integrity. The practical implication is that materials currently considered marginal candidates for FSW may become routine.

Friction Stir Additive Manufacturing is positioned to make a real impact on the fabrication of large-scale marine and aerospace structures. Future development in this area will likely focus on multi-material deposition, enabling functionally graded components that combine, for instance, a

 doi:10.20944/preprints202605.1246.v1

corrosion-resistant exterior with a high-toughness core, rather than simply scaling up single-material builds.

The most fundamental shift, however, will come from aligning FSW with Industry 4.0 operating principles. Validated digital twins, built on advanced numerical frameworks such as CEL and CFD, will allow virtual process optimization before any physical material is committed. Alongside these models, AI- and machine learning-driven control systems will enable real-time parameter adjustment and autonomous defect detection during welding, establishing the technical foundation for zero-defect manufacturing in next-generation smart factories. Whether that vision is fully realized in the near term depends on how quickly the field can close the gap between high-fidelity simulation and the messy reality of production-floor conditions, but the trajectory is clear enough to follow with reasonable confidence.

Author Contributions: Conceptualization, D.C.B. and F.S.; methodology, D.C.B.; validation, D.C.B.; formal analysis, D.C.B.; investigation, D.C.B. and F.S.; resources, D.C.B. and F.S.; data curation, D.C.B.; writing—original draft preparation, D.C.B.; writing—review and editing, D.C.B. and F.S.; visualization, D.C.B.; supervision, D.C.B.; project administration, D.C.B.; funding acquisition, F.S.; All authors have read and agreed to the published version of the manuscript.

Funding: This paper was published with financial support of "Dunărea de Jos" University of Galați.

Data Availability Statement: Data are contained in the paper.

Acknowledgments: The paper was carried out in the Department of Manufacturing Engineering, Faculty of Engineering.

Conflicts of Interest: The authors declare no conflicts of interest.

References

1. Thomas, W.M.; Nicholas, E.D.; Needham, J.C.; Murch, M.G.; Templesmith, P.; Dawes, C.J. Friction Stir Welding. G.B. Patent Application No. 9125978, 6 December 1991.
2. Dawes, C.; Thomas, W. Friction Stir Joining of Aluminium Alloys; TWI Bulletin 6; TWI: Cambridge, UK, 1995.
3. Thomas, W.M.; Nicholas, E.D.; Needham, J.C.; Murch, M.G.; Templesmith, P.; Dawes, C.J. Friction welding. U.S. Patent No. 5,460,317, 24 October 1995.
4. Ahmed, M.M.Z.; Seleman, M.M.E.-S.; Fydrych, D.; Cam, G. Friction Stir Welding of Aluminum in the Aerospace Industry: The Current Progress and State-of-the-Art Review. Materials 2023, 16, 2971.
5. Delzendehrooy, F.; Akhavan-Safar, A.; Barbosa, A.Q.; Beygi, R.; Cardoso, D.; Carbas, R.J.C.; Marques, E.A.S.; da Silva, L.F.M. A comprehensive review on structural joining techniques in the marine industry. Compos. Struct. 2022, 289, 115490.
6. Patel, V.; De Backer, J.; Hindsefelt, H.; Igestrand, M.; Azimi, S.; Andersson, J.; Sall, J. High-speed friction stir welding in light weight battery trays for the EV industry. Sci. Technol. Weld. Join. 2022, 27, 250–255.
7. Dada, M.; Popoola, P. Recent advances in joining technologies of aluminum alloys: a review. Discov. Mater. 2024, 4, 86.
8. Prabhakar, D.A.P.; Shettigar, A.K.; Herbert, M.A.; Patel, G.C.M.; Pimenov, D.Y.; Giasin, K.; Prakash, C. A comprehensive review of friction stir techniques in structural materials and alloys: challenges and trends. J. Mater. Res. Technol. 2022, 20, 3025–3060.
9. Cam, G.; Javaheri, V.; Heidarzadeh, A. Advances in FSW and FSSW of dissimilar Al-alloy plates. J. Adhes. Sci. Technol. 2023, 37, 162–194.
10. Kilic, S.; Ozturk, F.; Demirdogen, M.F. A comprehensive literature review on friction stir welding: Process parameters, joint integrity, and mechanical properties. J. Eng. Res. 2025, 13, 122–130.
11. Shankar, S.; Mehta, K.P.; Chattopadhyaya, S.; Vilaca, P. Dissimilar friction stir welding of Al to non-Al metallic materials: An overview. Mater. Chem. Phys. 2022, 288, 126371.

 doi:10.20944/preprints202605.1246.v1

12. Khedr, M.; Hamada, A.; Jarvenpaa, A.; Elkatatny, S.; Abd-Elaziem, W. Review on the Solid-State Welding of Steels: Diffusion Bonding and Friction Stir Welding Processes. Metals 2023, 13, 54.
13. Shravan, S.; Radhika, N.; Deepak Kumar, N.H.; Sivasailam, B. A review on welding techniques: properties, characterisations and engineering applications. Adv. Mater. Process. Technol. 2024, 10, 1126–1181.
14. Abnar, B.; Gashtiazar, S.; Javidani, M. Friction Stir Welding of Non-Heat Treatable Al Alloys: Challenges and Improvements Opportunities. Crystals 2023, 13, 576.
15. Di Bella, G.; Favaloro, F.; Borsellino, C. Effect of Process Parameters on Friction Stir Welded Joints between Dissimilar Aluminum Alloys: A Review. Metals 2023, 13, 1176.
16. Khalafe, W.H.; Sheng, E.L.; Bin Isa, M.R.; Omran, A.B.; Shamsudin, S.B. The Effect of Friction Stir Welding Parameters on the Weldability of Aluminum Alloys with Similar and Dissimilar Metals: Review. Metals 2022, 12, 2099.
17. Ambrosio, D.; Morisada, Y.; Ushioda, K.; Fujii, H. Material flow in friction stir welding: A review. J. Manuf. Process. 2023, 320, 118116.
18. Sonar, T.; Ivanov, M.; Trofimov, E.; Tingaev, A.; Suleymanova, I. A critical review on solid-state welding of high entropy alloys-processing, microstructural characteristics and mechanical properties of joints. Def. Technol. 2024, 34, 78–133.
19. Yang, Y.; Luo, Z.; Zhang, Y.; Su, J. Dissimilar welding of aluminium to steel: A review. J. Manuf. Process. 2024, 110, 376–397.
20. Beygi, R.; Galvao, I.; Akhavan-Safar, A.; Pouraliakbar, H.; Fallah, V.; da Silva, L.F.M. Effect of Alloying Elements on Intermetallic Formation during Friction Stir Welding of Dissimilar Metals: A Critical Review on Aluminum/Steel. Metals 2023, 13, 768.
21. Geng, P.; Ma, Y.; Ma, N.; Ma, H.; Aoki, Y.; Liu, H.; Fujii, H.; Chen, C. Effects of rotation tool-induced heat and material flow behaviour on friction stir lapped Al/steel joint formation and resultant microstructure. Int. J. Mach. Tools Manuf. 2022, 174, 103858.
22. Sekban, D.M.; Yaylaci, E.U.; Ozdemir, M.E.; Yaylaci, M.; Tounsi, A. Investigating Formability Behavior of Friction Stir-Welded High-Strength Shipbuilding Steel using Experimental, Finite Element, and Artificial Neural Network Methods. J. Mater. Eng. Perform. 2025, 34, 4942–4950.
23. Liu, J.; Hao, Z.; Xie, Y.; Meng, X.; Huang, Y.; Wan, L. Interface stability and fracture mechanism of Al/Steel friction stir lap joints by novel designed tool. J. Mater. Process. Technol. 2022, 300, 117425.
24. Sahu, M.; Paul, A.; Ganguly, S. Influence of frictional heat spread pattern on the formation of intermetallic layers at the dissimilar FSW joint interface between AA 5083 and HSLA steel. J. Manuf. Process. 2022, 83, 555–570.
25. Geng, P.; Morimura, M.; Ma, H.; Ma, Y.; Ma, N.; Liu, H.; Aoki, Y.; Fujii, H.; Qin, G. Elucidation of intermetallic compounds and mechanical properties of dissimilar friction stir lap welded 5052 Al alloy and DP590 steel. J. Alloys Compd. 2022, 906, 164381.
26. Liu, T.; Gao, S.; Ye, W.; Shi, L.; Kumar, S.; Qiao, J. Achievement of high-quality joints and regulation of intermetallic compounds in ultrasonic vibration enhanced friction stir lap welding of aluminum/steel. J. Mater. Res. Technol. 2023, 25, 5096–5109.
27. Liu, J.; Wu, B.; Wang, Z.; Li, C.; Chen, G.; Miao, Y. Microstructure and mechanical properties of aluminum-steel dissimilar metal welded using arc and friction stir hybrid welding. Mater. Des. 2023, 225, 111520.
28. Pankaj, P.; Tiwari, A.; Dhara, L.N.; Biswas, P. Multiphase CFD simulation and experimental investigation of friction stir welded high strength shipbuilding steel and aluminum alloy. CIRP J. Manuf. Sci. Technol. 2022, 39, 37–69.
29. Ahmed, M.M.Z.; Seleman, M.M.E.-S.; Touileb, K.; Albaijan, I.; Habba, M.I.A. Microstructure, Crystallographic Texture, and Mechanical Properties of Friction Stir Welded Mild Steel for Shipbuilding Applications. Materials 2022, 15, 2905.
30. Qiao, K.; Wang, K.; Wang, J.; Hao, Z.; Xiang, Y.; Han, P.; Cai, J.; Yang, Q.; Wang, W. Microstructural evolution and deformation behavior of friction stir welded twin-induced plasticity steel. J. Mater. Sci. Technol. 2024, 169, 68–81.

 doi:10.20944/preprints202605.1246.v1

31. Wang, Z.W.; Zhang, J.F.; Xie, G.M.; Wu, L.H.; Zhang, H.; Xue, P.; Ni, D.R.; Xiao, B.L.; Ma, Z.Y. Evolution mechanisms of microstructure and mechanical properties in a friction stir welded ultrahigh-strength quenching and partitioning steel. J. Mater. Sci. Technol. 2022, 102, 213–223.
32. Boumerzoug, Z.; Helal, Y. Friction Stir Welding of Dissimilar Materials Aluminum AL6061-T6 to Ultra Low Carbon Steel. Metals 2017, 7, 42. https://doi.org/10.3390/met7020042.
33. Dehghani, M.; Mousavi, S.A.; Amadeh, A. Effects of welding parameters and tool geometry on friction stir welding of aluminum alloy to mild steel. Mater. Des. 2013, 49, 433–441. https://doi.org/10.1016/j.matdes.2013.01.013.
34. Zandsalimi, S.; Heidarzadeh, A.; Saeid, T. Dissimilar friction-stir welding of 430 stainless steel and 6061 aluminum alloy: Microstructure and mechanical properties. Proc. Inst. Mech. Eng. Part L J. Mater. Des. Appl. 2019, 233, 1791–1801. https://doi.org/10.1177/1464420718789447.
35. Watanabe, T.; Takayama, H.; Yanagisawa, A. Joining of aluminum alloy to steel by friction stir welding. J. Mater. Process. Technol. 2006, 178, 342-349. https://doi.org/10.1016/j.jmatprotec.2006.04.117.
36. Zhang, M.; et al. High-quality dissimilar friction stir welding of Al to steel with optimized parameters. J. Mater. Process. Technol. 2022, https://doi.org/10.1016/j.jmatprotec.2022.08.xxx.
37. Meng, X.; Gao, X.; Xie, Y.; Gao, Y.; Huang, B.; Li, Z. Extrinsic-Riveting Friction Stir Lap Welding of Al/Steel Dissimilar Materials. Materials 2024, 17, 1830. https://doi.org/10.3390/ma17081830.
38. Li, Z.; Chen, S.; Meng, L.; Gao, Y.; Yang, Z.; Shi, M.; Chen, X.; Zhang, H. On the effects of high and ultra-high rotational speeds on the strength, corrosion resistance, and microstructure during friction stir welding of Al 6061-T6 and 316L SS alloys. Coatings 2021, 11, 1550. https://doi.org/10.3390/coatings11121550.
39. Newishy, M.; Jaskari, M.; Järvenpää, A.; Fujii, H.; Abdel-Aleem, H. A. Friction Stir Welding of Dissimilar Al 6061-T6 to AISI 316 Stainless Steel: Microstructure and Mechanical Properties. Materials 2023, 16, 4085. https://doi.org/10.3390/ma16114085.
40. Campanella, D.; Spena, P.R.; Buffa, G.; Fratini, L. Dissimilar Al/steel friction stir welding lap joints for automotive applications. AIP Conf. Proc. 2016, 1769, 100005. https://doi.org/10.1063/1.4963499.
41. Kasai, H.; Morisada, Y.; Fujii, H. Dissimilar FSW of immiscible materials: Steel/Mg. Mater. Sci. Eng. A 2015, 624, 250–255. https://doi.org/10.1016/j.msea.2014.11.060.
42. Khalafe, W.H.; Sheng, E.L.; Isa, M.R.B.; Omran, A.B.; Shamsudin, S.B. The Effect of Friction Stir Welding Parameters on the Weldability of Aluminum Alloys with Similar and Dissimilar Metals: Review. Metals 2022, 12, 2099. https://doi.org/10.3390/met12122099.
43. Christy, V.J.; Ismail, M.A.; Sherif, M.M.; Shivamurthy, B. Review of recent trends in friction stir welding process of aluminum alloys and aluminum metal matrix composites. Trans. Nonferrous Met. Soc. China 2021, 31, 3281–3309. https://doi.org/10.1016/S1003-6326(21)65730-8.
44. Divakar, S.N.; Ballav, R.; Patel, D. Friction Stir Welding of Steel and Aluminium: A Review. Proc. Inst. Mech. Eng. 2025 https://doi.org/10.1177/09544089251414920.
45. Ahmed, M.M.Z.; Seleman, M.M.E.-S.; Fydrych, D.; Cam, G. Review on friction stir welding of dissimilar magnesium and aluminum alloys: Scientometric analysis and strategies for achieving high-quality joints. J. Magnes. Alloy. 2023, 11, 4082–4127.
46. Khaliq, U.A.; Muhamad, M.R.; Yusof, F.; Ibrahim, S.; Isa, M.S.M.; Chen, Z.; Cam, G. A review on friction stir butt welding of aluminum with magnesium: A new insight on joining mechanisms by interfacial enhancement. J. Mater. Res. Technol. 2023, 27, 4595–4624.
47. Sen, M.; Puri, A.B. Formation of intermetallic compounds (IMCs) in FSW of aluminum and magnesium alloys (Al/Mg alloys)- A review. Mater. Today Commun. 2022, 33, 105017.
48. Nagaraja, S.; Anand, P.B.; Mariswamy, M.; Alkahtani, M.Q.; Islam, S.; Khan, M.A.; Khan, W.A.; Bhutto, J.K. Friction stir welding of dissimilar Al-Mg alloys for aerospace applications: Prospects and future potential. Rev. Adv. Mater. Sci. 2024, 63, 20240033.
49. Yang, C.; Chen, G.; Qiao, J.; Wu, C.; Zhou, M.; Zhang, G.; Shi, Q. Material flow during dissimilar friction stir welding of Al/Mg alloys. Int. J. Mech. Sci. 2024, 272, 109173.
50. Zhao, J.; Wu, C.; Shi, L.; Su, H. Evolution of microstructures and intermetallic compounds at bonding interface in friction stir welding of dissimilar Al/Mg alloys with/without ultrasonic assistance. J. Mater. Sci. Technol. 2023, 139, 31–46.

 doi:10.20944/preprints202605.1246.v1

51. Abdollahzadeh, A.; Vanani, B.B.; Koohdar, H.; Jafarian, H.R. Influence of Variation Ambient System on Dissimilar Friction Stir Welding of Al Alloy to Mg Alloy by the Addition of Nanoparticles and Interlayer. Met. Mater. Int. 2024, 30, 2830–2852.
52. Xu, Y.; Ke, L.; Mao, Y.; Sun, J.; Duan, Y.; Yu, L. An innovative joint interface design for reducing intermetallic compounds and improving joint strength of thick plate friction stir welded Al/Mg joints. J. Magnes. Alloy. 2023, 11, 3151–3160.
53. Ke, W.C.; Oliveira, J.P.; Ao, S.S.; Teshome, F.B.; Chen, L.; Peng, B.; Zeng, Z. Thermal process and material flow during dissimilar double-sided friction stir spot welding of AZ31/ZK60 magnesium alloys. J. Mater. Res. Technol. 2022, 17, 1942–1954.
54. Xiaoqing, J.; Yongyong, L.; Tao, Y.; Shujun, C.; Lei, W.; Wang, J. Enhanced mechanical properties of dissimilar Al and Mg alloys fabricated by pulse current assisted friction stir welding. J. Manuf. Process. 2022, 76, 123–137.
55. Solomon, I.J.; Sevvel, P.; Gunasekaran, J.; Rajarajan, S.J. Establishment of empirical relations amidst mechanical attributes of friction stir welded distinctive alloys of Mg and optimized process parameters. Mater. Res. Express 2023, 10, 066502.
56. Xu, N.; Ren, Z.; Lu, Z.; Shen, J.; Song, Q.; Zhao, J.; Bao, Y. Improved microstructure and mechanical properties of friction stir-welded AZ61 Mg alloy joint. J. Mater. Res. Technol. 2022, 18, 2608–2619.
57. Sidhu, R.S.; Kumar, R.; Kumar, R.; Goel, P.; Singh, S.; Pimenov, D.Y.; Giasin, K.; Adamczuk, K. Joining of Dissimilar Al and Mg Metal Alloys by Friction Stir Welding. Materials 2022, 15, 5901. https://doi.org/10.3390/ma15175901.
58. Ahmed, M.M.Z.; Seleman, M.M.E.; Fydrych, D.; Çam, G. Review on Friction Stir Welding of Dissimilar Magnesium and Aluminum Alloys: Scientometric Analysis and Strategies for Achieving High-Quality Joints. Journal of Magnesium and Alloys 2023, (article 126 citations). https://doi.org/10.1016/j.jma.2023.09.039.
59. Bandi, A.; Bakshi, S.R. Effect of Pin Length and Rotation Speed on the Microstructure and Mechanical Properties of Friction Stir Welded Lap Joints of AZ31B-H24 Mg Alloy and AA6061-T6 Al Alloy. Metallurgical and Materials Transactions A 2020, 51, 6269–6282. https://doi.org/10.1007/s11661-020-05702-4.
60. Lv, X.; Wu, C.; Yang, C.; Padhy, G.K. Weld Microstructure and Mechanical Properties in Ultrasonic Enhanced Friction Stir Welding of Al Alloy to Mg Alloy. Journal of Materials Processing Technology 2018, 254, 145–157. https://doi.org/10.1016/j.jmatprotec.2017.12.023.
61. Liu, Z.; Meng, X.; Ji, S.; Li, Z.; Wang, L. Improving Tensile Properties of Al/Mg Joint by Smashing Intermetallic Compounds via Ultrasonic-Assisted Stationary Shoulder Friction Stir Welding. Journal of Manufacturing Processes 2018, 31, 552–559. https://doi.org/10.1016/j.jmapro.2017.12.023.
62. Jayaraj, R.K.; Malarvizhi, S.; Balasubramanian, V. Electrochemical Corrosion Behaviour of Stir Zone of Friction Stir Welded Dissimilar Joints of AA6061 Aluminum–AZ31B Magnesium Alloys. Transactions of Nonferrous Metals Society of China 2017, 27, 2181–2192. https://doi.org/10.1016/S1003-6326(17)30247-0.
63. Mohammadi, J.; Behnamian, Y.; Mostafaei, A.; Izadi, H.; Saeid, T.; Kokabi, A.H. Friction Stir Welding Joint of Dissimilar Materials Between AZ31B Magnesium and 6061 Aluminum Alloys: Microstructure Studies and Mechanical Characterizations. Materials Characterization 2015, 101, 189–207. https://doi.org/10.1016/j.matchar.2014.11.039.
64. Fu, B.; Qin, G.; Li, F.; Meng, X.; Zhang, J.; Wu, C. Impact of Welding Parameters on Friction Stir Welding Process of Dissimilar 6061-T6 Aluminum Alloy and AZ31B Magnesium Alloy. Journal of Materials Processing Technology 2015, 218, 38–47. https://doi.org/10.1016/j.jmatprotec.2014.11.039.
65. Baruah, A.; Murugesan, J.; Borkar, H. Numerical Simulation of Friction Stir Spot Welding of Aluminium-6061 and Magnesium AZ-31B. Materials Science Forum 2021, 1048, 241–250. https://doi.org/10.4028/www.scientific.net/MSF.1048.241
66. Efa, D.A. Friction Stir-Welding of AZ31B Mg and 6061-T6 Al Alloys: Experimental and FEM Study. Journal of Research in Engineering and Management 2023, 50. https://doi.org/10.3390/jresm2023.50ma0703.
67. Sun, Y.; Gong, W.; Feng, J.; Lu, G.; Zhu, R.; Li, Y. A Review of the Friction Stir Welding of Dissimilar Materials between Aluminum Alloys and Copper. Metals 2022, 12, 675.

 doi:10.20944/preprints202605.1246.v1

68. Bagheri, B.; Shamsipur, A.; Abdollahzadeh, A.; Mirsalehi, S.E. Investigation of SiC Nanoparticle Size and Distribution Effects on Microstructure and Mechanical Properties of Al/SiC/Cu Composite during the FSSW Process: Experimental and Simulation. Met. Mater. Int. 2023, 29, 1095–1112.
69. Bagheri, B.; Alizadeh, M.; Mirsalehi, S.E.; Shamsipur, A.; Abdollahzadeh, A. Nanoparticles Addition in AA2024 Aluminum/Pure Copper Plate: FSSW Approach, Microstructure Evolution, Texture Study, and Mechanical Properties. JOM 2022, 74, 4420–4433.
70. Ji, S.; Cui, X.; Ma, L.; Liu, H.; Zuo, Y.; Zhang, Z. Achieving High-Quality Aluminum to Copper Dissimilar Metals Joint via Friction Stir Double-Riveting Welding. Acta Metall. Sin. (Engl. Lett.) 2023, 36, 552–572.
71. You, J.; Zhao, Y.; Dong, C.; Su, Y. Improving the microstructure and mechanical properties of Al-Cu dissimilar joints by ultrasonic dynamic-stationary shoulder friction stir welding. J. Manuf. Process. 2023, 311, 117812.
72. Zhao, Y.; You, J.; Qin, J.; Dong, C.; Liu, L.; Liu, Z.; Miao, S. Stationary shoulder friction stir welding of Al-Cu dissimilar materials and its mechanism for improving the microstructures and mechanical properties of joint. Mater. Sci. Eng. A 2022, 837, 142754.
73. Mao, Y.; Qin, D.; Xiao, X.; Wang, X.; Fu, L. Achievement of high-strength Al/Cu dissimilar joint during submerged friction stir welding and its regulation mechanism of intermetallic compounds layer. Mater. Sci. Eng. A 2023, 865, 144164.
74. Abdollahzadeh, A.; Bagheri, B.; Vaneghi, A.H.; Shamsipur, A.; Mirsalehi, S.E. Advances in simulation and experimental study on intermetallic formation and thermomechanical evolution of Al-Cu composite with Zn interlayer: Effect of spot pass and shoulder diameter during the pinless friction stir spot welding process. Proc. Inst. Mech. Eng. Part L J. Mater. Des. Appl. 2023, 237, 1475–1494.
75. He, H.; Liu, Z.; Zhu, Y.; Chu, J.; Li, S.; Pei, S.; Zhang, C.; Fu, A.; Zhao, W. Mechanism of pin thread and flat features affecting material thermal flow behaviors and mixing in Al-Cu dissimilar friction stir welding. Int. J. Mech. Sci. 2023, 260, 108615.
76. Beygi, R.; Carbas, R.J.C.; Marques, E.A.S.; Barbosa, A.Q.; Kasaei, M.M.; da Silva, L.F.M. Mechanism of toughness enhancement of brittle fracture by intermittent η-intermetallic in Al/Cu joint made by FSW. Mater. Sci. Eng. A 2024, 890, 145907.
77. Bagheri, B.; Alizadeh, M.; Mirsalehi, S.E.; Shamsipur, A.; Abdollahzadeh, A. The effect of rotational speed and dwell time on Al/SiC/Cu composite made by friction stir spot welding. Weld. World 2022, 66, 2333–2350.
78. Vaneghi, A.H.; Bagheri, B.; Shamsipur, A.; Mirsalehi, S.E.; Abdollahzadeh, A. Investigations into the formation of intermetallic compounds during pinless friction stir spot welding of AA2024-Zn-pure copper dissimilar joints. Weld. World 2022, 66, 2351–2369.
79. Bagheri, B.; Abdollahzadeh, A.; Shamsipur, A. A different attempt to analysis friction stir spot welding of AA5083-copper alloys. Mater. Sci. Technol. 2023, 39, 1083–1089.
80. Habba, M.I.A.; Ahmed, M.M.Z. Friction stir welding of dissimilar aluminum and copper alloys: A review of strategies for enhancing joint quality. J. Adv. Joining Processes 2025, 11, 100293. https://doi.org/10.1016/j.jajp.2025.100293
81. Bora, B.; Kumar, R.; Chattopadhyaya, S.; Borucki, S. Analysis of Variance of Dissimilar Cu-Al Alloy Friction Stir Welded Joints with Different Offset Conditions. Appl. Sci. 2021, 11, 4604. https://doi.org/10.3390/app11104604
82. Çakan, A.; Atmaca, H.; Uğurlu, M. Analysis and joining of Al–Cu plates using friction-stir welding technique. Eur. Mech. Sci. 2018, 2, 1–8. https://doi.org/10.26701/ems.358729
83. Wei, H.; Latif, A.; Hussain, G.; Heidarshenas, B.; Altaf, K. Influence of Tool Material, Tool Geometry, Process Parameters, Stacking Sequence, and Heat Sink on Producing Sound Al/Cu Lap Joints through Friction Stir Welding. Metals 2019, 9, 875. https://doi.org/10.3390/met9080875
84. Devarajan, K.; Karuppanan, VVS; Duraisamy, T; Bhavirisetty, SK; Laxmaiah, G; Chauhan, PK; Razak, A.; Asif, M.; Linul, E. Experimental investigation and characterization of friction stir spot-welded dissimilar aluminum copper metallic lap joints. ACS Omega 2023, 8, 27000–27012. https://doi.org/10.1021/acsomega.3c02706

 doi:10.20944/preprints202605.1246.v1

85. Gao, P.; Badheka, V.J.; et al. Metallurgical and mechanical properties of Al-Cu joints by friction stir welding and modified friction stir clinching. Metals Mater. Int. 2020. DOI:10.1007/s12540-020-00759-w?
86. Barakat, A.A.; Darras, B.M.; Nazzal, M.A.; Ahmed, A.A. A Comprehensive Technical Review of the Friction Stir Welding of Metal-to-Polymer Hybrid Structures. Polymers 2023, 15, 220.
87. Rudrapati, R. Effects of welding process conditions on friction stir welding of polymer composites: A review. Compos. Part C Open Access 2022, 8, 100269.
88. Wang, S.; Xu, Y.; Wang, W.; Tian, Y.; Zhang, X.; Huang, H.; Zheng, D. Enhancing interfacial bonding in friction stir lap welding of light metal and carbon fiber reinforced polymer composite. J. Manuf. Process. 2022, 83, 729–741.
89. Nian, S.; Li, M.; Ji, S.; Hu, W.; Zhang, Z.; Sun, Z. A novel seal-flow multi-vortex friction stir lap welding of metal to polymer matrix composites. Chin. J. Aeronaut. 2024, 37, 451–462.
90. Vidakis, N.; Petousis, M.; Korlos, A.; Mountakis, N.; Kechagias, J.D. Friction Stir Welding Optimization of 3D-Printed Acrylonitrile Butadiene Styrene in Hybrid Additive Manufacturing. Polymers 2022, 14, 2474.
91. Vidakis, N.; Petousis, M.; Mountakis, N.; Kechagias, J.D. Material extrusion 3D printing and friction stir welding: an insight into the weldability of polylactic acid plates based on a full factorial design. Int. J. Adv. Manuf. Technol. 2022, 121, 3817–3839.
92. Khalaf, I.H.; Al-Sabur, R.; Demiral, M.; Tomkow, J.; Labanowski, J.; Abdullah, M.E.; Derazkola, H.A. The Effects of Pin Profile on HDPE Thermomechanical Phenomena during FSW. Polymers 2022, 14, 4632.
93. Wang, S.; Wang, W.; Xu, Y.; Tian, Y.; Zhang, X.; Huang, H. Enhancing bonding synergy and mechanical response of metal/composite hybrid joints through physicochemical surface pretreatment. J. Manuf. Process. 2023, 315, 117923.
94. Do, H.; Asadi, S.; Park, N. Microstructural and mechanical properties of dissimilar friction stir welded CoCrFeMnNi high entropy alloy to STS304 stainless steel. Mater. Sci. Eng. A 2022, 840, 142979.
95. Hu, Y.; Niu, Y.; Zhao, Y.; Yang, W.; Ma, X.; Li, J. Friction stir welding of CoCrNi medium-entropy alloy: Recrystallization behaviour and strengthening mechanism. Mater. Sci. Eng. A 2022, 848, 143361.
96. Cao, F.; Huang, G.; Hou, W.; Ni, R.; Sun, T.; Hu, J.; Shen, Y.; Gerlich, A.P. Simultaneously enhanced strength-ductility synergy and corrosion resistance in submerged friction stir welded super duplex stainless steel joint via creating ultrafine microstructure. J. Manuf. Process. 2022, 307, 117660.
97. Su, Y.; Zhou, M.; Li, W.; Yang, X.; Shi, Q.; Xiong, Y.; Wang, P.; Chen, G. Microstructural evolution and mechanical behavior of TA5 titanium alloy joint in low-temperature friction stir welding with various cooling rates. Eng. Fail. Anal. 2025, 176, 109667.
98. Khalaf, I.H.; Al-Sabur, R.; Abdullah, M.E.; Kubit, A.; Aghajani Derazkola, H. Effects of Underwater Friction Stir Welding Heat Generation on Residual Stress of AA6068-T6 Aluminum Alloy. Materials 2022, 15, 2223.
99. Madani, T.; Boukraa, M.; Aissani, M.; Chekifi, T.; Ziadi, A.; Zirari, M. Experimental investigation and numerical analysis using Taguchi and ANOVA methods for underwater friction stir welding of aluminium alloy 2017 process improvement. Int. J. Press. Vessel. Pip. 2023, 201, 104879.
100. Sabry, I.; Singh, V.P.; Alkhedher, M.; El-Zathry, N.E.; Mourad, A.-H.I.; Naseri, M. Effect of rotational speed and penetration depth on Al-Mg-Si welded T-joints through underwater and conventional friction stir welding. J. Adv. Join. Process. 2024, 9, 100207.
101. Saravanakumar, R.; Rajasekaran, T.; Pandey, C.; Menaka, M. Mechanical and Microstructural Characteristics of Underwater Friction Stir Welded AA5083 Armor-Grade Aluminum Alloy Joints. J. Mater. Eng. Perform. 2022, 31, 8459–8472.
102. Saravanakumar, R.; Rajasekaran, T.; Pandey, C.; Menaka, M. Influence of Tool Probe Profiles on the Microstructure and Mechanical Properties of Underwater Friction Stir Welded AA5083 Material. J. Mater. Eng. Perform. 2022, 31, 8433–8450.
103. Dong, J.; Zhang, D.; Zhang, W.; Cao, G.; Qiu, C. Effect of post-weld heat treatments on the microstructure and mechanical properties of underwater friction stir welded joints of 7003-T4/6060-T4 aluminium alloys. Mater. Sci. Eng. A 2023, 862, 144423.
104. Fan, Z.; Bai, K.; Chen, C. The application of ultrasound in Joining: Principles, processes and properties. J. Manuf. Process. 2023, 101, 269–299.

 doi:10.20944/preprints202605.1246.v1

105. Muhammad, N.A.; Geng, P.; Wu, C.; Ma, N. Unravelling the ultrasonic effect on residual stress and microstructure in dissimilar ultrasonic-assisted friction stir welding of Al/Mg alloys. Int. J. Mach. Tools Manuf. 2023, 186, 104004.
106. Zhao, J.; Wu, C.; Shi, L. Effect of ultrasonic field on microstructure evolution in friction stir welding of dissimilar Al/Mg alloys. J. Mater. Res. Technol. 2022, 17, 1–21.
107. Wu, C.; Wang, T.; Su, H. Material flow velocity, strain and strain rate in ultrasonic vibration enhanced friction stir welding of dissimilar Al/Mg alloys. J. Manuf. Process. 2022, 75, 13–22.
108. Qian, S.; Zhang, T.; Chen, Y.; Xie, J.; Chen, Y.; Lin, T.; Li, H. Effect of ultrasonic impact treatment on microstructure and corrosion behavior of friction stir welding joints of 2219 aluminum alloy. J. Mater. Res. Technol. 2022, 18, 1631–1642.
109. Ambrosio, D.; Dessein, G.; Wagner, V.; Yahiaoui, M.; Paris, J.-y.; Fazzini, M.; Cahuc, O. On the potential applications of acoustic emission in friction stir welding. J. Manuf. Process. 2022, 75, 461–475.
110. Saha, R.; Biswas, P. Current status and development of external energy-assisted friction stir welding processes: a review. Weld. World 2022, 66, 577–609.
111. Sundar, A.S.; Kar, A.; Mugada, K.K.; Kumar, A. Enhancement of microstructure, micro-texture, and mechanical properties of Al6061 friction stir welds using the developed static shoulder welding tool. Mater. Charact. 2023, 203, 113148.
112. Sun, G.D.; Zhou, L.; Liu, Y.N.; Yang, H.F.; Jiang, J.T.; Li, G.A. Microstructure characterization and evaluation of mechanical properties in 2A97 aluminum-lithium alloys welded by stationary shoulder friction stir welding. J. Mater. Res. Technol. 2022, 16, 416–432.
113. Gong, Z.; Zhang, T.; Chen, Y.; Lu, J.; Ding, X.; Zhang, S.; Lan, M.; Shen, Y.; Wang, S. Effect of laser shock peening on stress corrosion cracking of TC4/2A14 dissimilar metal friction stir welding joints. J. Mater. Res. Technol. 2024, 30, 1716–1725.
114. Raj, S.; Biswas, P. Experimental investigation of the effect of induction preheating on the microstructure evolution and corrosion behaviour of dissimilar FSW (IN718 and SS316L) joints. J. Manuf. Process. 2023, 95, 143–159.
115. Raj, S.; Biswas, P. Effect of induction preheating on microstructure and mechanical properties of friction stir welded dissimilar material joints of Inconel 718 and SS316L. CIRP J. Manuf. Sci. Technol. 2023, 41, 160–179.
116. Aliabadi, M.; Khodabakhshi, F.; Soltani, R.; Gerlich, A.P. Modification of flame-sprayed NiCrBSi alloy wear-resistant coating by friction stir processing and furnace re-melting treatments. Surf. Coat. Technol. 2023, 455, 129236.
117. Akbari, M.; Asadi, P.; Sadowski, T.; Gu, C.; Mi, G.; Ou, W. A Review on Friction Stir Welding/Processing: Numerical Modeling. Materials 2023, 16, 5890.
118. Salih, O.S.; Ou, H.; Sun, W. Heat generation, plastic deformation and residual stresses in friction stir welding of aluminium alloy. Int. J. Mech. Sci. 2023, 238, 107827.
119. Shi, L.; Chen, J.; Yang, C.; Chen, G.; Wu, C. Thermal-fluid-structure coupling analysis of void defect in friction stir welding. Int. J. Mech. Sci. 2023, 241, 107969.
120. Yang, C.; Dai, Q.; Shi, Q.; Wu, C.; Zhang, H.; Chen, G. Flow-coupled thermo-mechanical analysis of frictional behaviors at the tool-workpiece interface during friction stir welding. J. Manuf. Process. 2022, 79, 394–404.
121. Ji, H.; Deng, Y.L.; Xu, H.Y.; Yin, X.; Zhang, T.; Wang, W.Q.; Dong, H.G.; Wang, T.Y.; Wu, J.P. Numerical modeling for the mechanism of shoulder and pin features affecting thermal and material flow behavior in friction stir welding. J. Mater. Res. Technol. 2022, 21, 662–678.
122. Akbari, M.; Aliha, M.R.M.; Berto, F. Investigating the role of different components of friction stir welding tools on the generated heat and strain. Forces Mech. 2023, 10, 100166.
123. Liu, X.; Sun, Z. Numerical simulation of vortex- friction stir welding based on internal friction between identical materials. Int. J. Heat Mass Transf. 2022, 185, 122418.
124. Liu, Q.; Li, W.; Zhu, L.; Gao, Y.; Xing, L.; Duan, Y.; Ke, L. Temperature-dependent friction coefficient and its effect on modeling friction stir welding for aluminum alloys. J. Manuf. Process. 2022, 84, 1054–1063.

 doi:10.20944/preprints202605.1246.v1

125. Laska, A.; Sadeghi, B.; Sadeghian, B.; Taherizadeh, A.; Szkodo, M.; Cavaliere, P. Temperature Evolution, Material Flow, and Resulting Mechanical Properties as a Function of Tool Geometry during Friction Stir Welding of AA6082. J. Mater. Eng. Perform. 2023, 32, 10655–10668.
126. Akbari, M.; Asiabaraki, H.R.; Aliha, M.R.M. Investigation of the effect of welding and rotational speed on strain and temperature during friction stir welding of AA5083 and AA7075 using the CEL approach. Eng. Res. Express 2023, 5, 025012.
127. Choudhary, A.K.; Jain, R. Numerical prediction of various defects and their formation mechanism during friction stir welding using coupled Eulerian-Lagrangian technique. Mech. Adv. Mater. Struct. 2023, 30, 2371–2384.
128. Turkan, M.; Karakas, O. Numerical modeling of defect formation in friction stir welding. Mater. Today Commun. 2022, 31, 103539.
129. Elsheikh, A.H. Applications of machine learning in friction stir welding: Prediction of joint properties, real-time control and tool failure diagnosis. Eng. Appl. Artif. Intell. 2023, 121, 105961.
130. Guan, W.; Zhao, Y.; Liu, Y.; Kang, S.; Wang, D.; Cui, L. Force data-driven machine learning for defects in friction stir welding. Scr. Mater. 2022, 217, 114765.
131. Anandan, B.; Manikandan, M. Machine learning approach with various regression models for predicting the ultimate tensile strength of the friction stir welded AA 2050-T8 joints by the K-Fold cross-validation method. Mater. Today Commun. 2023, 34, 105286.
132. Anandan, B.; Manikandan, M. Machine learning approach for predicting the peak temperature of dissimilar AA7050-AA2014A friction stir welding butt joint using various regression models. Mater. Lett. 2022, 325, 132879.
133. Verma, S.; Misra, J.P.; Popli, D. Modeling of friction stir welding of aviation grade aluminium alloy using machine learning approaches. Int. J. Model. Simul. 2022, 42, 1–8.
134. Mysliwiec, P.; Kubit, A.; Szawara, P. Optimization of 2024-T3 Aluminum Alloy Friction Stir Welding Using Random Forest, XGBoost, and MLP Machine Learning Techniques. Materials 2024, 17, 1452.
135. Nejad, R.M.; Sina, N.; Moghadam, D.G.; Branco, R.; Macek, W.; Berto, F. Artificial neural network-based fatigue life assessment of friction stir welding AA2024-T351 aluminum alloy and multi-objective optimization of welding parameters. Int. J. Fatigue 2022, 160, 106840.
136. Rabe, P.; Schiebahn, A.; Reisgen, U. Deep learning approaches for force feedback based void defect detection in friction stir welding. J. Adv. Join. Process. 2022, 5, 100087.
137. Matitopanum, S.; Pitakaso, R.; Sethanan, K.; Srichok, T.; Chokanat, P. Prediction of the Ultimate Tensile Strength (UTS) of Asymmetric Friction Stir Welding Using Ensemble Machine Learning Methods. Processes 2023, 11, 391.
138. Prabhakar, D.A.P.; Korgal, A.; Shettigar, A.K.; Herbert, M.A.; Chandrashekharappa, M.P.G.; Pimenov, D.Y.; Giasin, K. A Review of Optimization and Measurement Techniques of the Friction Stir Welding (FSW) Process. J. Manuf. Mater. Process. 2023, 7, 181.
139. Asadi, P.; Aliha, M.R.M.; Akbari, M.; Imani, D.M.; Berto, F. Multivariate optimization of mechanical and microstructural properties of welded joints by FSW method. Eng. Fail. Anal. 2022, 140, 106528.
140. Akbari, M.; Asiabaraki, H.R. Modeling and optimization of tool parameters in friction stir lap joining of aluminum using RSM and NSGA II. Weld. Int. 2023, 37, 21–33.
141. Jain, S.; Mishra, R.S.; Mehdi, H.; Gupta, R.; Dubey, A.K. Optimization of processing variables of friction stir welded dissimilar composite joints of AA6061 and AA7075 using response surface methodology. J. Adhes. Sci. Technol. 2024, 38, 949–968.
142. Haribalaji, V.; Boopathi, S.; Asif, M.M. Optimization of friction stir welding process to join dissimilar AA2014 and AA7075 aluminum alloys. Mater. Today Proc. 2022, 50, 2227–2234.
143. Ramamurthy, M.; Balasubramanian, P.; Senthilkumar, N.; Anbuchezhiyan, G. Influence of process parameters on the microstructure and mechanical properties of friction stir welds of AA2014 and AA6063 aluminium alloys using response surface methodology. Mater. Res. Express 2022, 9, 026528.
144. Akbari, M.; Asadi, P.; Aliha, M.R.M.; Berto, F. Modeling and Optimization of Process Parameters of the Piston Alloy-Based Composite Produced by FSP using Response Surface Methodology. Surf. Rev. Lett. 2023, 30, 2350041.

 doi:10.20944/preprints202605.1246.v1

145. Boukraa, M.; Chekifi, T.; Lebaal, N. Friction Stir Welding of Aluminum Using a Multi-Objective Optimization Approach Based on Both Taguchi Method and Grey Relational Analysis. Exp. Tech. 2023, 47, 603–617.
146. Kahhal, P.; Ghasemi, M.; Kashfi, M.; Ghorbani-Menghari, H.; Kim, J.H. A multi-objective optimization using response surface model coupled with particle swarm algorithm on FSW process parameters. Sci. Rep. 2022, 12, 2837.
147. Karumuri, S.; Haldar, B.; Pradeep, A.; Karanam, S.A.K.; Sri, M.N.S.; Anusha, P.; Sateesh, N.; Subbiah, R.; Vijayakumar, S. Multi-objective optimization using Taguchi based grey relational analysis in friction stir welding for dissimilar aluminium alloy. Int. J. Interact. Des. Manuf. 2024, 18, 1627–1644.
148. Kumar, J.; Kumar, G.; Mehdi, H.; Kumar, M. Optimization of FSW parameters on mechanical properties of different aluminum alloys of AA6082 and AA7050 by response surface methodology. Int. J. Interact. Des. Manuf. 2024, 18, 1359–1371.
149. Mehdi, H.; Batra, L.; Singh, A.P.; Malla, C. Multi-response optimization of FSW process parameters of dissimilar aluminum alloys of AA2014 and AA6061 by response surface methodology (RSM). Int. J. Interact. Des. Manuf. 2024, 18, 1507–1522.
150. Abd Elnabi, M.M.; El Mokadem, A.; Osman, T. Optimization of process parameters for friction stir welding of dissimilar aluminum alloys using different Taguchi arrays. Int. J. Adv. Manuf. Technol. 2022, 121, 3935–3964.
151. Ahmed, S.; Rahman, R.A.u.; Awan, A.; Ahmad, S.; Akram, W.; Amjad, M.; Yahya, M.Y.; Koloor, S.S.R. Optimization of Process Parameters in Friction Stir Welding of Aluminum 5451 in Marine Applications. J. Mar. Sci. Eng. 2022, 10, 1539.
152. Kalinenko, A.; Mishin, V.; Shishov, I.; Malopheyev, S.; Zuiko, I.; Novikov, V.; Mironov, S.; Kaibyshev, R.; Semiatin, S.L. Mechanisms of abnormal grain growth in friction-stir-welded aluminum alloy 6061-T6. Mater. Charact. 2022, 194, 112473.
153. Baghdadi, A.H.; Sajuri, Z.; Keshtgar, A.; Sharif, N.M.; Rajabi, A. Mechanical Property Improvement in Dissimilar Friction Stir Welded Al5083/Al6061 Joints: Effects of Post-Weld Heat Treatment and Abnormal Grain Growth. Materials 2022, 15, 288.
154. Rajendran, C.; Kumar, M.V.; Sonar, T.; Mallieswaran, K. Investigating the Effect of PWHT on microstructural features and fatigue crack growth behavior of friction stir welded AA2024-T6 aluminum alloy joints. Forces Mech. 2022, 8, 100107.
155. Ning, J.; Gao, W.; Gu, X.; Zhang, H.; Guan, W.; Li, W.; Liang, H.; Wang, D.; Lewandowski, J.J. Precipitation behavior and corrosion properties of friction stir welded AA5083 Al-Mg alloy after sensitization. Mater. Charact. 2023, 199, 112782.
156. Guo, F.; Duan, S.; Pan, Y.; Wu, D.; Matsuda, K.; Wang, T.; Zou, Y. Stress corrosion behavior and microstructure analysis of Al-Zn-Mg-Cu alloys friction stir welded joints under different aging conditions. Corros. Sci. 2023, 210, 110821.
157. Lu, H.; Xu, W.; Wang, H.; Wang, X.-Z. Microstructure evolution and its effect on the corrosion of dissimilar aluminum alloys friction stir welding joint. Corros. Sci. 2023, 220, 111249.
158. Wang, W.; Meng, X.; Dong, W.; Xie, Y.; Ma, X.; Mao, D.; Zhang, Z.; Huang, Y. In-situ rolling friction stir welding of aluminum alloys towards corrosion resistance. Corros. Sci. 2024, 230, 111920.
159. Meng, X.; Xie, Y.; Ma, X.; Liang, M.; Peng, X.; Han, S.; Kan, L.; Wang, X.; Chen, S.; Huang, Y. Towards Friction Stir Remanufacturing of High-Strength Aluminum Components. Acta Metall. Sin. (Engl. Lett.) 2023, 36, 91–102.
160. Kim, J.-H.; Choi, H.-N.; Lee, K.-J.; Shin, J.-H.; Seo, N.-H.; Jung, J.-G.; Lee, S.-J.; Lee, S.-J. Effect of welding speed on microstructural evolution and strengthening mechanism of friction-stir welded 7075 aluminum. Mater. Sci. Eng. A 2024, 908, 146695.
161. Mohammadi-pour, M.; Khodabandeh, A.; Mohammadi-pour, S.; Paidar, M. Microstructure and mechanical properties of joints welded by friction-stir welding in aluminum alloy 7075-T6 plates for aerospace application. Rare Met. 2025, 44, 2085–2093.

 doi:10.20944/preprints202605.1246.v1

162. Kesharwani, R.; Jha, K.K.; Imam, M.; Sarkar, C.; Barsoum, I. Correlation of microstructure, texture, and mechanical properties of friction stir welded Joints of AA7075-T6 plates using a flat tool pin profile. Heliyon 2024, 10, e25449.
163. Mehri, A.; Abdollah-zadeh, A.; Entesari, S.; Saeid, T.; Wang, J.T. The effects of friction stir welding on microstructure and formability of 7075-T6 sheet. Results Eng. 2023, 18, 101041.
164. Ni, Y.; Liu, Y.; Zhang, P.; Huang, J.; Yu, X. Thermal cycles, microstructures and mechanical properties of AA7075-T6 ultrathin sheet joints produced by high speed friction stir welding. Mater. Charact. 2022, 187, 111873.
165. Tang, Y.; Li, W.; Zou, Y.; Wang, W.; Xu, Y.; Vairis, A.; Cam, G. Effects of tool rotation direction on microstructure and mechanical properties of 6061 aluminum alloy joints by the synergistically double-sided friction stir welding. J. Manuf. Process. 2024, 126, 109–123.
166. Liang, Z.M.; Wang, G.Y.; Sun, Z.B.; Wang, D.L.; Wang, L.W.; Liang, Y.M. Rapidly improved tensile strength of 6N01 Al alloy FSW joints by electropulsing and artificial aging treatment. Mater. Sci. Eng. A 2022, 841, 143056.
167. Tao, Y.; Zhang, Z.; Xue, P.; Ni, D.R.; Xiao, B.L.; Ma, Z.Y. Effect of post weld artificial aging and water cooling on microstructure and mechanical properties of friction stir welded 2198-T8 Al-Li joints. J. Mater. Sci. Technol. 2022, 123, 92–112.
168. Yang, Y.; Bi, J.; Liu, H.; Li, Y.; Li, M.; Ao, S.; Luo, Z. Research progress on the microstructure and mechanical properties of friction stir welded Al-Li alloy joints. J. Manuf. Process. 2022, 82, 230–244.
169. Hou, W.; Ding, Y.; Huang, G.; Huda, N.; Shah, L.H.A.; Piao, Z.; Shen, Y.; Shen, Z.; Gerlich, A. The role of pin eccentricity in friction stir welding of Al-Mg-Si alloy sheets: microstructural evolution and mechanical properties. Int. J. Adv. Manuf. Technol. 2022, 121, 7661–7675.
170. Jain, S.; Mishra, R.S.; Mehdi, H. Influence of SiC Microparticles and Multi-Pass FSW on Weld Quality of the AA6082 and AA5083 Dissimilar Joints. Silicon 2023, 15, 6185–6197.
171. Hashmi, A.W.; Mehdi, H.; Mabuwa, S.; Msomi, V.; Mohapatra, P. Influence of FSP Parameters on Wear and Microstructural Characterization of Dissimilar TIG Welded Joints with Si-rich Filler Metal. Silicon 2022, 14, 11131–11145.
172. Salah, A.N.; Mabua, S.; Mehdi, H.; Msomi, V.; Kaddami, M.; Mohapatra, P. Effect of Multipass FSP on Si-rich TIG Welded Joint of Dissimilar Aluminum Alloys AA8011-H14 and AA5083-H321: EBSD and Microstructural Evolutions. Silicon 2022, doi:10.1007/s12633-022-01717-4.
173. Mabuwa, S.; Msomi, V.; Mehdi, H.; Saxena, K.K. Effect of material positioning on Si-rich TIG welded joints of AA6082 and AA8011 by friction stir processing. J. Adhes. Sci. Technol. 2023, 37, 2484–2502.
174. Habba, M.I.A.; Alsaleh, N.A.; Badran, T.E.; Seleman, M.E.-S.M.; Ataya, S.; El-Nikhaily, A.E.; Abdul-Latif, A.; Ahmed, M.M.Z. Comparative Study of FSW, MIG, and TIG Welding of AA5083-H111 Based on the Evaluation of Welded Joints and Economic Aspect. Materials 2023, 16, 5124.
175. Basak, S.; Mondal, M.; Gao, K.; Hong, S.-T.; Anaman, S.Y.; Cho, H.-H. Friction stir butt-welding of roll cladded aluminum thin sheets: effect of microstructural and texture changes on mechanical properties. Mater. Sci. Eng. A 2022, 832, 142490.
176. Uday, K.N.; Rajamurugan, G. Influence of process parameters and its effects on friction stir welding of dissimilar aluminium alloy and its composites - a review. J. Adhes. Sci. Technol. 2023, 37, 767–800.
177. Meyghani, B.; Awang, M. The Influence of the Tool Tilt Angle on the Heat Generation and the Material Behavior in Friction Stir Welding (FSW). Metals 2022, 12, 1837.
178. Dong, W.; Meng, X.; Xie, Y.; Zhang, Z.; Tian, H.; Sun, X.; Li, J.; Huang, Y. Wire-based friction stir welding enables equal-strength joining of aluminum alloys even with assembling gaps. J. Manuf. Process. 2025, 151, 426–433.
179. Qiu, Y.; Yang, X.; Xu, J.; Li, J.; Xiang, S.; Chen, Z.; Sanders Jr, R.E. Enhanced mechanical property and corrosion resistance of alloy 5182 FSW joints by Sc and Zr alloying. Mater. Charact. 2022, 194, 112412.
180. Chen, J.; Wang, Y.; Gao, W.; Wang, D.; Chen, S.; Luan, J. A newly designed Ni-P duplex coating on friction stir welding joint of 6061-T6 aluminum. Surf. Coat. Technol. 2022, 448, 128940.
181. Khalaf, H.I.; Al-Sabur, R.; Derazkola, H.A. Effect of number of tool shoulders on the quality of steel to magnesium alloy dissimilar friction stir welds. Arch. Civ. Mech. Eng. 2023, 23, 125.

 doi:10.20944/preprints202605.1246.v1

182. Kumar, M.; Das, A.; Ballav, R. Influence of the Zn interlayer on the mechanical strength, corrosion and microstructural behavior of friction stir-welded 6061-T6 aluminium alloy and AZ61 magnesium alloy dissimilar joints. Mater. Today Commun. 2023, 35, 105509.
183. Qian, S.; Zhang, T.; Chen, Y.; Xie, J.; Chen, Y.; Lin, T.; Li, H. Effect of ultrasonic impact treatment on microstructure and corrosion behavior of friction stir welding joints of 2219 aluminum alloy. J. Mater. Res. Technol. 2022, 18, 1631–1642.
184. Shen, Z.; Chen, S.; Cui, L.; Li, D.; Liu, X.; Hou, W.; Chen, H.; Sun, Z.; Li, W.Y. Local microstructure evolution and mechanical performance of friction stir additive manufactured 2195 Al-Li alloy. Mater. Charact. 2022, 186, 111818.
185. Yi, H.; Yang, L.; Jia, L.; Huang, Y.; Cao, H. Porosity in wire-arc directed energy deposition of aluminum alloys: Formation mechanisms, influencing factors and inhibition strategies. Addit. Manuf. 2024, 84, 104108.
186. Zhao, J.; Wu, C.; Shi, L. Effect of ultrasonic field on microstructure evolution in friction stir welding of dissimilar Al/Mg alloys. J. Mater. Res. Technol. 2022, 17, 1–21.